



**CALIFORNIA
ENERGY COMMISSION**



ENERGY RESEARCH AND DEVELOPMENT DIVISION

FINAL PROJECT REPORT

Integrated Distributed Fiber-Optic Sensing for Real-time Monitoring of Offshore Wind Turbine Gearboxes, Tower Operations, and Marine Animal Activities

May 2025 | CEC-500-2025-023

PREPARED BY:

Yuxin Wu Linqing Luo
Lawrence Berkeley National Laboratory

Kenichi Soga Matthew DeJong
Jaewon Saw James Xu
University of California, Berkeley
Primary Authors

Mark Danielson
Project Manager
California Energy Commission

Agreement Number: EPC-19-010

Kevin Uy
Branch Manager
ENERGY SUPPLY BRANCH

Jonah Steinbuck, Ph.D.
Director
ENERGY RESEARCH AND DEVELOPMENT DIVISION

Drew Bohan
Executive Director

DISCLAIMER

This report was prepared as the result of work sponsored by the California Energy Commission (CEC). It does not necessarily represent the views of the CEC, its employees, or the State of California. The CEC, the State of California, its employees, contractors, and subcontractors make no warranty, express or implied, and assume no legal liability for the information in this report; nor does any party represent that the uses of this information will not infringe upon privately owned rights. This report has not been approved or disapproved by the CEC, nor has the California Energy Commission passed upon the accuracy or adequacy of the information in this report.

ACKNOWLEDGEMENTS

This project was made possible through the support and funding provided by the California Energy Commission. We extend our deepest gratitude to the California Energy Commission for recognizing both the importance of advancing monitoring technologies in the renewable energy sector and for its commitment to fostering innovative research that addresses critical environmental challenges.

We would like to acknowledge the invaluable contributions from our project partners, including the University of California, Berkeley, Siemens Gamesa, and the Monterey Bay Aquarium Research Institute. Their combined expertise, facilities, and collaboration were instrumental in the successful execution of this project. Special thanks are extended to our colleague at the National Renewable Energy Laboratory for its support and contributions to our joint research activities at their National Wind Technology Center.

We also thank the industry stakeholders, wind developers, and regulatory agencies that engaged with us throughout this research. Their insights and feedback were crucial in shaping our research outcomes that meet real-world needs.

Finally, we are grateful to all the researchers, technicians, and students who dedicated their time and expertise to this project. Their hard work, innovation, and commitment to excellence were vital in achieving the project's objectives.

PREFACE

The California Energy Commission's (CEC) Energy Research and Development Division supports energy research and development programs to spur innovation in energy efficiency, renewable energy and advanced clean generation, energy-related environmental protection, energy transmission, and distribution and transportation.

In 2012, the Electric Program Investment Charge (EPIC) was established by the California Public Utilities Commission to fund public investments in research to create and advance new energy solutions, foster regional innovation, and bring ideas from the lab to the marketplace. The EPIC Program is funded by California utility customers under the auspices of the California Public Utilities Commission. The CEC and the state's three largest investor-owned utilities—Pacific Gas and Electric Company, San Diego Gas and Electric Company, and Southern California Edison Company—were selected to administer the EPIC funds and advance novel technologies, tools, and strategies that provide benefits to their electric ratepayers.

The CEC is committed to ensuring public participation in its research and development programs that promote greater reliability, lower costs, and increase safety for the California electric ratepayer and include:

- Providing societal benefits.
- Reducing greenhouse gas emission in the electricity sector at the lowest possible cost.
- Supporting California's loading order to meet energy needs first with energy efficiency and demand response, next with renewable energy (distributed generation and utility scale), and finally with clean, conventional electricity supply.
- Supporting low-emission vehicles and transportation.
- Providing economic development.
- Using ratepayer funds efficiently.

Integrated Distributed Fiber-Optic Sensing for Real-time Monitoring of Offshore Wind Turbine Gearboxes, Tower Operations, and Marine Animal Activities is the final report for Contract Number EPC-19-010 conducted by Lawrence Berkeley National Laboratory and the University of California, Berkeley. The information from this project contributes to the Energy Research and Development Division's Electric Program Investment Charge Program.

For more information about the Energy Research and Development Division, please visit the [CEC's research website \(www.energy.ca.gov/research/\)](http://www.energy.ca.gov/research/) or contact the Energy Research and Development Division at ERDD@energy.ca.gov.

ABSTRACT

Floating offshore wind systems offer a promising potential to expand renewable energy generation by utilizing deep ocean wind resources. However, the deployment of these systems requires advanced monitoring techniques to ensure structural integrity and minimize environmental impacts. This project, funded by the California Energy Commission, provided enhanced monitoring of floating offshore wind systems by integrating distributed fiber-optic sensing technologies. This research focused on three key areas: monitoring wind tower integrity, assessing gearbox performance with high-resolution strain measurements, and detecting marine mammal activity using distributed acoustic sensing.

The experiments demonstrated that distributed fiber-optic sensing technologies could effectively monitor strain profiles in wind towers and gearboxes in addition to providing detailed operation monitoring and early detection of potential failures. Distributed acoustic sensing was validated as a non-invasive tool for detecting whale vocalizations, although challenges related to noise mitigation were identified. The project's knowledge transfer activities facilitated dissemination of findings through scholarly publications, industry collaborations, and government engagement, establishing a foundation for future research and technology adoption.

Overall, this project advanced state-of-the-art technology for floating offshore wind monitoring and contributed to the development of safer and more environmentally responsible offshore wind-energy systems. Recommendations include continued stakeholder engagement, refinement of monitoring techniques, and adaptive strategies that support broader deployment of distributed fiber-optic sensing technologies in the offshore wind-energy sector.

Keywords: Floating offshore wind (FOSW), distributed fiber optic sensing (DFOS), distributed acoustic sensing (DAS)

Please use the following citation for this report:

Wu Y., L. Luo, K. Soga, M. DeJong, J. Saw, and J. Xu. 2024. *Integrated Distributed Fiber-Optic Sensing for Real-Time Monitoring of Offshore Wind Turbine Gearboxes, Tower Operations, and Marine Animal Activities – Final Project Report*. California Energy Commission. Publication Number: CEC-500-2025-023.

TABLE OF CONTENTS

Acknowledgements	i
Preface.....	ii
Abstract	iii
Executive Summary.....	1
Background	1
Project Purpose and Approach	1
Key Results.....	2
Knowledge Transfer and Next Steps.....	3
Conclusion and Recommendations	3
CHAPTER 1: Introduction	5
Importance of Monitoring FOSW Systems.....	5
Project Scope and Focus.....	5
Current State of Knowledge and Technological Maturity	6
Project Goals and Metrics for Success.....	6
Benefits to California Ratepayers.....	6
CHAPTER 2: Project Approach	8
Technical Tasks	8
Task 1: Initial Technological Evaluation	8
Task 2: Development of an Advanced Laboratory Testing Facility.....	9
Task 3: Laboratory Studies to Validate Technology Feasibility	9
Task 4: Developing Numerical Capabilities for Data Collection, Processing, Analysis and Visualization	10
Task 5: Controlled Failure Experiments and Associated FOS Signals	10
Task 6: Numerical Approach Improvements Based on Failure Mode Experiments	10
Task 7: Field Test Planning and Preparation	11
Task 8: Field Demonstration	11
Task 9: Evaluation of Project Benefits	11
Project Partners and Participants.....	12
Key Project Milestones.....	12
Summary.....	13
CHAPTER 3: Results.....	15
Wind Tower Monitoring	15
Technologies Used	15
Four-Point Bend Test.....	15
Shake Table Test	17
Key Technical Barriers	18
Key Results.....	18
Summary.....	23

Gearbox Operation Monitoring	24
Experimental Setup	24
Key Technical Barriers	24
Solutions to the Barriers	24
Key Results.....	25
Summary.....	30
Marine Mammal Detection at Monterey Bay	30
Experimental Setup	31
Key Results.....	39
CHAPTER 4: Conclusion.....	41
Key Findings	41
Benefits to California Ratepayers.....	41
Future Research and Recommendations	42
Strengthening Industry and Academic Collaborations	42
Engagement With Policymakers	42
Conclusion.....	43
Glossary and List of Acronyms	44
References	46
Project Deliverables.....	48
Appendix A: Data Summary Table.....	A-1

LIST OF FIGURES

Figure 1: Fiber-Optic Installation Layout (in Red) for the 4-Point Bend Test (Side View)	16
Figure 2: Turbine Being Loaded With Weights During the 4-Point Bend Test.....	16
Figure 3: View of Wind Turbine on the Shake Table, From the Base.....	17
Figure 4: Fiber-Optic Installation Layout (in Red) for the Shake Table Test (Side View)	17
Figure 5: Axial Strain for Bolt Configuration 1, With Theoretical Strains Plotted	19
Figure 6: Circumferential Strain for All Bolt Configurations.....	20
Figure 7: Strain Envelope Comparisons for Bolt Configuration 1	21
Figure 8: ϕ -OTDR Strain Time Series During the Translational Loading Configuration for Bolt Configuration 1	22
Figure 9: Averaged PSD Values for Longitudinal Channels in the Bottom Section of Axis 3 Using Φ -OTDR Data During Translational Shaking (With Tilt).....	23
Figure 10: Waterfall Representation of the Strain Profile Over Time for the Circumference of the Ring Rear	25

Figure 11: Strain Response After 0.01-Hz High-pass at Location 4.62 M	26
Figure 12: Strain Profile in Polar Axis and the Strain Versus Torque Input.....	27
Figure 13: Strain Reading at Different Locations Versus Time and Torque Inputs.....	28
Figure 14: Strain and Temperature Reading Profiles in the Field Test	29
Figure 15: Peak-to-peak Strain With Input Torque and Output Power in the Field Test.....	30
Figure 16: Research Vessel in Monterey Bay With DAS Interrogator Housed Inside the Cabin and DAS Cable Lowered to the Water Using A-Frame.....	31
Figure 17: Magnitude Spectra and Spectrograms Compared From Raw DAS Data, Showing the Impacts of Boat Engine Noise and Cable Location on the Noise Floor and the Visibility of Signals	32
Figure 18: Time Series Adjusted to Visualize Whale Vocalizations – the Signal Recorded at Approximately 6 Seconds Was a Whale Vocalization.	34
Figure 19: Schematic of Experimental Setup	35
Figure 20: Schematic of Configuration With Buoy at an Intermediate Location Along the Cable	35
Figure 21: Schematic of Configuration With Loops Along the Cable at Different Depths.....	36
Figure 22: Magnitude Spectra and Spectrograms From the Raw DAS Data	36
Figure 23: Spectrogram Generated From DAS Data When a Pre-Recorded Whale Song Was Played on the Underwater Speaker Before and After Median-Filtering	38
Figure 24: DAS Capture of Pre-Recorded Whale Song	39
Figure 25: Examples of Natural Whale Vocalizations Captured by DAS.....	40

LIST OF TABLES

Table 1: Four-Point Bend Test Loading Configurations Used for Each Bolt Configuration.....	16
Table 2: Shake Table Test Loading Configurations Used for Each Bolt Configuration	18
Table 3: Shake Test Averaged PSDs For Each Bolt Configuration During Loading Configuration 2	23
Table A-1: Distributed Strain and Temperature Sensing (including Wind Turbine Structure Tests and Gearbox Monitoring Tests)	A-1
Table A-2: Distributed Acoustic Sensing (including Wind Turbine Structure Tests and Whale Calling Recording Tests).....	A-1

Executive Summary

Background

Floating offshore wind (FOSW) will provide a valuable resource for achieving the clean energy goals of Senate Bill 100 and for supporting grid reliability. Additionally, Assembly Bill 525 requires the California Energy Commission to develop a strategic plan for offshore wind energy developments in federal waters off the coast of California and establish megawatt planning goals for 2030 and 2045. In 2021, the Department of the Interior, the Department of Defense, and the State of California announced an agreement to advance areas for FOSW energy development off the northern and the central coasts. In December 2022, the Bureau of Ocean Energy Management awarded two leases for the Humboldt wind energy area and three leases for the Morro Bay wind energy area, which together have the potential to generate over four gigawatts of offshore wind energy. Together, these five leases represent important first steps in the build-out of a significant domestic clean energy resource.

The anticipated development and deployment of FOSW systems on the California coast will require evaluation of a diverse array of potential environmental impacts, such as changes to marine life populations, habitat, oceanic processes (e.g., upwelling, nutrient flux), and collision and entanglement risks. The potential impacts from such installations are not well documented and will require site-specific evaluations at the wind energy areas, due to the novelty of both floating installations and their interaction with California ecosystems. Current environmental monitoring technologies face limitations in the temporal and spatial resolution and coverage, accuracy, and durability needed to adequately represent the risks and impacts. Additionally, continuous monitoring and data collection may be needed to better understand risks from FOSW systems to natural resources and wildlife.

This research project advanced distributed fiber-optic sensing (DFOS) technologies for the real-time monitoring of turbines and gearboxes under simulated operating conditions and for monitoring of marine mammal activities. This will be critically important to ensure the environmentally sustainable development of this industry, now in its infancy. This research project's benefits include reducing operations and maintenance costs, providing greater reliability and safety, and detecting potential environmental impacts. The project's objectives focused on evaluating the technical feasibility of DFOS technologies for FOSW turbine tower and gearbox operation and integrity monitoring, detecting marine mammal activities, and improving the technology readiness of DFOS to support deployment of FOSW systems in coastal California.

Project Purpose and Approach

The primary goal of this project was to develop a novel, distributed, high-resolution fiber optical sensing system based on Rayleigh and Brillouin backscattering for real-time monitoring of gearbox and tower operation and marine-mammal activities near offshore wind turbines, based on three-dimensional strain, vibration, and temperature monitoring. The project was

focused on experimental validation and was structured around the following three key experiments:

1. **Wind Tower Monitoring:** This experiment, conducted under simulated offshore conditions, utilized both optical frequency domain reflectometry (OFDR) and ϕ -optical time domain reflectometry (ϕ -OTDR) to detect strain profiles and dynamics in wind towers.
2. **Gearbox Operation Monitoring:** This experiment used DFOS technologies to measure gearbox strain distributions under various load conditions. Separate collaborations with Siemens Gamesa and the National Renewable Energy Laboratory enabled testing of DFOS technologies on modern production gearboxes. Experimental data was analyzed to quantify torque inputs and detect potential faults, offering a significant improvement over traditional point sensors.
3. **Marine Mammal Detection:** Distributed acoustic sensing was deployed to detect whale vocalizations in Monterey Bay, California, to evaluate the use of distributed acoustic sensing as a tool to measure the impact of FOSW systems on marine life. Experimental data was compared with hydrophone recordings to validate the effectiveness of distributed acoustic sensing in noisy marine environments.

Key Results

The experiments demonstrated significant advancements in the safety, reliability, and environmental monitoring of FOSW systems using DFOS technologies, with the following direct implications for both industry and academic research.

- **Structural Health Monitoring:** The application of DFOS was successful in capturing both dynamic and static strain profiles and offered critical insights into the structural behavior of wind towers. ϕ -OTDR was highly effective in detecting high-frequency strain events, making it ideal for large-scale offshore monitoring. These outcomes represent a substantial advancement for the wind energy industry by demonstrating, for the first time, new tools for real-time monitoring, which enhances the operational safety and longevity of offshore wind turbines. For academia, this research contributes valuable data for the future development of numerical algorithms and structural analysis models.
- **Gearbox Performance:** DFOS provided detailed, real-time strain measurements across the entire gearbox housing (as opposed to traditional point sensors), enabling early detection of faults and accurate torque predictions, which are essential for proactive maintenance. The continuous, high-resolution monitoring capability marks a breakthrough in gearbox health management for floating offshore wind turbines, where access for physical inspections is limited. For the wind energy sector, these findings demonstrate the potential for reducing costly downtimes and improving overall turbine efficiency; for researchers, it opens new possibilities for optimizing gearbox design and maintenance strategies, using real-time data.

- **Environmental Impact Assessment:** The experiments demonstrated, for the first time, that DFOS can effectively detect whale vocalizations under the ocean's challenging noise conditions, confirming its utility as a non-invasive tool for marine mammal vocalization monitoring. This finding is particularly relevant for developers and regulators seeking to understand the environmental impacts of offshore wind projects on marine mammals. Additionally, it provides researchers with a new platform for exploring marine ecosystem dynamics and improving noise mitigation strategies that ensure more accurate and reliable environmental assessments.

Knowledge Transfer and Next Steps

A knowledge transfer plan was executed to disseminate project results through scholarly publications, public reports, and active engagement with industry and regulatory stakeholders. Key activities follow.

- **Publications and Outreach:** The project team published its findings in peer-reviewed journals and presented at international conferences. The project team also conducted outreach to other researchers and institutions, setting the stage for future research in such areas as integrating artificial intelligence for data analysis and enhancing offshore wind-structure durability.
- **Industry and Government Engagement:** Discussions with offshore wind developers, research institutions, and government agencies aligned research outputs with industry needs and fostered partnerships for future technology deployment. Engagements with the United States Department of Energy and other agencies raised awareness of the project's contributions to national renewable energy and environmental goals. Collaborations with Siemens Gamesa and other industry leaders facilitated practical testing and validation of DFOS technologies.

Conclusion and Recommendations

The successful development of DFOS technologies in this project marks a significant step toward the deployment of remote, real-time monitoring systems capable of assessing the structural integrity of offshore wind turbines, particularly their gearboxes and towers. The project demonstrated that DFOS technologies can provide continuous, high-resolution data crucial for detecting early signs of wear, fatigue, and potential failures in critical components. This capability is essential for maintaining the reliability and safety of FOSW systems, especially in remote and harsh marine environments where manual inspections are both costly and challenging. Additionally, the project advanced marine mammal detection capabilities by using DFOS to monitor whale vocalizations, promoting environmentally responsible development of offshore wind facilities. Potential ratepayer benefits from this project include greater electricity reliability, lower costs, and increased safety by providing real-time equipment monitoring to track operations and diagnose prefailure signs.

The project results underscore the effectiveness of DFOS technologies in enhancing structural health monitoring and environmental impact assessments, but further advancements are needed to stimulate commercial deployment. Specifically, future work should focus on

improving the robustness and scalability of DFOS systems for large-scale offshore applications. In particular, the integration of DFOS with turbine control systems for automated, real-time adjustments (based on strain and torque data) is a critical next step. Additionally, improving distributed acoustic sensing noise mitigation techniques is essential for enhancing the accuracy of marine mammal detection in dynamic and noisy ocean environments. These technical capabilities must be advanced to move DFOS technologies closer to commercial adoption. Targeted efforts in refining these methodologies, combined with continued collaboration with industry stakeholders, will be crucial in driving the deployment of reliable, cost-effective, and environmentally sustainable FOSW systems.

CHAPTER 1:

Introduction

Floating offshore wind (FOSW) is a rapidly evolving renewable energy resource that enables wind turbines to be sited in deep ocean waters where traditional fixed-bottom foundations are not feasible. By utilizing floating platforms anchored to the seabed, FOSW systems can access the stronger, more consistent wind resources found in deeper waters, offering a significant opportunity to expand renewable wind energy generation. This technology minimizes visual and environmental impacts compared to nearshore wind farms, making it especially relevant for regions with deep-water coastlines, such as those in California.

California's deep offshore waters, coupled with the state's ambitious renewable energy mandates (Senate Bill 100 and Assembly Bill 525), make FOSW an important component of the state's future renewable energy mix. The potential benefits of FOSW include harnessing substantial clean energy from offshore winds, creating jobs in engineering and construction, and solidifying California's leadership in renewable-energy technologies.

Importance of Monitoring FOSW Systems

The successful deployment of FOSW systems hinges not only on technological innovation but also on robust FOSW equipment monitoring and environmental impact monitoring. This monitoring data will support proactive maintenance to reduce downtimes, improve capacity factors, and evaluate and mitigate environmental impacts. In California, where these systems will be located miles from shore in deep waters subjected to harsh conditions, strong currents, and seismic activity, monitoring becomes even more critical. Structural health monitoring of key components such as wind towers and gearboxes is necessary to detect early signs of wear, mitigate risks, and ensure safe, long-term reliability.

In addition to structural health, environmental monitoring is essential for minimizing potential impacts on marine life. FOSW systems can generate noise and vibrations, which may disrupt marine ecosystems, particularly affecting marine mammals like whales. Advanced monitoring techniques help detect and mitigate these impacts, ensuring that FOSW developments are both technologically sound and environmentally responsible.

Project Scope and Focus

This project aimed to enhance monitoring capabilities for FOSW system operations and marine mammal activities through the development of innovative fiber-optic sensing technologies. It focused on the following three primary areas:

1. **Wind Tower Monitoring:** Developing advanced techniques for monitoring the structural health of wind towers using DFOS to detect dynamic and static strain profiles under simulated offshore conditions.

2. **Gearbox Operation Monitoring:** Implementing high-resolution strain measurement techniques to monitor gearbox performance and predict potential failures. This is critical for offshore systems where opportunities and access for maintenance is limited.
3. **Marine Mammal Detection:** Exploring the use of DAS to detect whale vocalizations and assessing the environmental impacts of FOSW installations on marine mammals.

Current State of Knowledge and Technological Maturity

FOSW is an emerging technology that faces both technical and environmental challenges. Traditional monitoring approaches using point sensors are often inadequate in providing enough spatial resolution to identify integrity issues early enough for proactive maintenance actions to be taken. Distributed fiber-optic sensing (DFOS) offers continuous, high-resolution strain measurements, providing detailed insights into the structural behavior of wind towers and gearboxes, while distributed acoustic sensing (DAS) represents a novel approach to environmental monitoring capable of detecting acoustic signals over long distances.

While DFOS and DAS have shown promise in other industries, their application in FOSW monitoring requires further validation under real-world conditions. This project bridges that gap by advancing these technologies for offshore wind facilities.

Project Goals and Metrics for Success

Primary project goals included:

- **Improving Structural Health Monitoring:** Developing robust methodologies using DFOS to monitor wind tower and gearbox performance, with quantitative metrics of 1-10 microstrain sensitivity, spatial resolution of less than 3 millimeters and sampling frequency of greater than 10 hertz.
- **Assessing Environmental Impacts:** Validating DAS technology for detecting marine mammal vocalizations, with metrics evaluating signal detection capabilities and noise mitigation effectiveness.
- **Advancing Market Adoption:** Demonstrating the feasibility of these monitoring technologies to industry stakeholders to encourage broader adoption in commercial FOSW projects.

Benefits to California Ratepayers

This project benefits California ratepayers by improving the safety, reliability, and environmental sustainability of FOSW systems. By advancing monitoring technologies, this project enables real-time, remote monitoring of wind turbine structures, reducing the need for costly and time-consuming manual inspections. These monitoring technologies reduce operations and maintenance costs (estimated at one-third of the levelized cost of energy [LCOE]) and minimize the likelihood of unplanned system failures, which in turn leads to lower energy costs for Californians. Additionally, the proactive maintenance capabilities enabled by DFOS reduce the risk of catastrophic failures, further enhancing reliability and safety. DAS, by

monitoring environmental impacts on marine life, also supports the environmentally responsible deployment of offshore wind projects, benefiting ratepayers through timely and sustainable energy production.

CHAPTER 2:

Project Approach

This chapter describes the methodologies and overall strategy used to achieve the project objectives. The project was organized around the three following overarching components:

- (1) Desktop studies on baseline technology evaluations.
- (2) Numerical capability developments and data analysis, presentations, and technology demonstrations (in both lab and field settings).
- (3) Project benefits and technology transfer activities.

The baseline technology evaluation provided information on current state-of-the-art design studies and approaches to testing at both lab and field scales. The project resulted in improvements to the state-of-the-art design and provided the basis for discussing the project's benefits and technology transfer activities. This chapter focuses on the first and second components just described; the third component is summarized in Chapter 4: Conclusion.

The project team followed a set of tasks around these three main components; the discussion of this approach focuses on nine technical tasks.

Technical Tasks

Task 1: Initial Technological Evaluation

This task focused on understanding the critical issues facing offshore wind turbine (OWT) components — evaluating technologies for monitoring the performance of these components and assessing their ability to detect marine mammal activities. The project team conducted a literature review and evaluated the feasibility of using DFOS technologies for the continuous monitoring of key OWT components like gearboxes and towers, where traditional point-sensor-based systems have limited application. DFOS can detect strain, vibration, temperature, and acoustic changes in real time, preventing damage and reducing maintenance costs through predictive maintenance strategies. The feasibility of using DFOS for the acoustic monitoring of marine mammal activities was also explored, since it offers a potential solution for monitoring the environmental impacts to large mammals (whales) from floating offshore wind facilities. The work done in this task concluded that DFOS is a promising tool for monitoring both the operational performance of floating offshore wind turbines (FOWTs) and their potential impacts on marine mammal activities, supporting both cost reduction and sustainability goals. This task provided a baseline survey of the current state-of-the-art technology and the type of facilities needed to test the project's DFOS technology innovations.

Task 2: Development of an Advanced Laboratory Testing Facility

Based on the previous task, which established the need for advanced experimentation, the goal of this task was to design and construct a laboratory test facility to conduct technology performance testing and evaluation under relevant offshore wind conditions. This task used the facility to develop and demonstrate the usage of DFOS technologies for real-time monitoring of OWT structural health, reducing the need for manual inspections. The specific goal was to test the capability of DFOS systems to detect potential failures in the wind turbine under both static and dynamic loading conditions, to both improve reliability and lower operation and maintenance costs. This test facility is centered around a 6-degree-of-freedom large shake table¹ to induce simulated motions of wind turbines under offshore conditions.

Two key tests were conducted at the test facility: a static load test and a dynamic shake table test. In the static test, loads were applied incrementally to a wind turbine tower while DFOS systems measured strain. In the dynamic test, the wind turbine was subjected to simulated ground motions to mimic the conditions of an offshore floating platform; different DFOS technologies — Rayleigh and Brillouin scattering-based systems — were used to capture strain data. The experiments were carried out in the following tasks. The main conclusion was that DFOS technology shows promise for accurately monitoring the health of OWTs in real time, which could significantly improve the maintenance process and reduce downtimes. Task 2 set up the experimental capability to support the subsequent tasks (Task 3 and Task 5) and associated other tasks (Task 4 and Task 6).

Task 3: Laboratory Studies to Validate Technology Feasibility

This task features one of the main experiments and is described in more detail in the next chapter. The main work conducted during this task involved large-scale laboratory tests using a 65-kilowatt (kW) Nordtank wind turbine tower. The tower was subjected to a bend test (under quasi-static conditions) and a shake-table test that simulated multidirectional loads representative of offshore wind environments. Two fiber-optic sensing technologies were used to measure strain responses; the results showed good agreement between the two sensing methods. The tests confirmed that the technology could accurately capture dynamic strain profiles and localized strain phenomena over large distances, making it a promising technology for OWT structural health monitoring. Key lessons on effective installation techniques were also identified.

Through collaboration with Siemens Gamesa, another experiment was conducted to evaluate the performance of DFOS for monitoring strain and temperature changes in wind turbine gearboxes under operational conditions. The test results demonstrated that DFOS technologies could effectively monitor the real-time health of wind-turbine gearboxes by detecting early warning signs of potential mechanical issues, which is critical to reducing maintenance costs and minimizing turbine downtimes. The experimental results from this task supported development of the numerical capabilities in the next task.

¹ Six degrees of freedom refers to the six independent ways a rigid body can move in three-dimensional space. This means that the shake table can translate linearly along the x-axis (forward/back), y-axis (left/right), or z-axis (up/down) as well as rotate around each axis (pitch, roll, or yaw).

Task 4: Developing Numerical Capabilities for Data Collection, Processing, Analysis and Visualization

Utilizing data gathered from the previous task, the focus of this task was the development of data processing, analysis, and visualization capabilities for datasets generated from experiments conducted during the project. The main goals included development and implementation of advanced numerical processes to handle large datasets collected from DFOS technologies. In the case of OWT structural monitoring, new methods for strain conversion, frequency mode analysis, and spectral analysis were applied to detect changes such as tower bending or bolt loosening. For marine mammal detection, adaptive filtering, temporal segmentation, and bandpass filtering were used to isolate whale calls from noise in challenging underwater acoustic environments. This task demonstrated how these numerical processes enable real-time, high-precision monitoring, which improved both predictive maintenance capabilities and accurate detection of whale calls.

Task 5: Controlled Failure Experiments and Associated FOS Signals

Based on the previous experiments, this task focused on controlled failure experiments (using the lab test facility to simulate damage scenarios such as loose bolts and tower deformation) to fully understand associated DFOS signals. The tests focused on monitoring real-time strain changes and detecting structural anomalies under varying operational conditions. In the case of loose bolt detection, the work involved simulating dynamic loading and recording strain data during both free and forced vibration tests. By systematically loosening bolts, the project team evaluated how strain profiles and natural frequencies of the structure change, allowing it to pinpoint the impact of these modifications on the wind turbine's overall integrity.

The tests also examined both bending strain and axial strain by positioning DFOS sensors along different sections of the wind turbine tower. These sensors captured the deflection and bending moments that occur under simulated loads, particularly when the top nacelle (the enclosure housing the drivetrain and other essential components of the turbine) and blades introduced external forces. By integrating strain data over time and applying frequency mode analysis, the tests offered insights into how specific controlled failures, such as bolt loosening, affected the overall behavior of the wind turbine. The comprehensive strain and frequency analyses served as early indicators of structural degradation, allowing for timely maintenance interventions and improvements in predictive health monitoring of the wind turbines. The results from this task were key to numerical approach improvements described in the next task.

Task 6: Numerical Approach Improvements Based on Failure Mode Experiments

This task focused on improving data-processing methodologies for monitoring wind turbine structural integrity and marine mammal activity, using experiment results from the previous task. For the structural integrity assessment, the focus was on detecting bolt loosening through frequency-mode analysis. Strain data from optical frequency domain reflectometry (OFDR) revealed frequency shifts corresponding to different damage states, with a decrease in

peak natural frequency, which indicates loosening bolts. Consistent strain patterns across the turbine structure validated this method for the early detection of structural vulnerabilities.

For marine mammal monitoring, DAS technology was optimized to address environmental noise challenges. Advanced signal processing methods, such as adaptive filtering and bandpass filtering, improved detection of whale calls by isolating relevant frequencies from background noise. Temporal segmentation allowed for more precise analysis of acoustic events. These enhancements in data processing contributed to more accurate monitoring of both wind turbine health and marine ecosystems, highlighting the utility and value of DFOS and DAS technologies in offshore wind and environmental applications.

Task 7: Field Test Planning and Preparation

The focus of this task was planning and preparing for the field tests to validate the performance of DFOS technologies for monitoring the structural integrity of both OWTs and their environmental impacts, particularly on marine mammals. Given the absence of operational FOSW farms in the United States, the field tests simulated real-world conditions using alternative environments.

The field tests were planned across three key areas. For the wind turbine tower, a smaller-scale turbine was placed on a shake table to simulate a range of operational conditions, allowing the DFOS technologies to capture data on strain and structural behaviors. The gearbox testing took place at Siemens Gamesa's facility in Spain, where DFOS monitored strain and temperature in a real-world gearbox system. For environmental monitoring, the project deployed DAS technology in the Monterey Bay National Marine Sanctuary to detect whale calls, working closely with marine researchers. These field tests were essential for validating the reliability and effectiveness of using DFOS and DAS technologies in operational and environmental contexts.

Task 8: Field Demonstration

The results showed that DFOS and DAS technologies can effectively monitor both turbine performance and the presence of marine mammals. Field tests also demonstrated the ability of DFOS to capture strain data from wind turbine structures, including bolt loosening and gearbox operation. DAS successfully recorded whale calls, although there were challenges related to noise interference from vessel engines and environmental factors. Overall, research indicated that DFOS and DAS could play a crucial role in both enhancing turbine reliability and minimizing marine environmental impacts, with further refinement required for noise management and signal processing.

In addition to the technical tasks just described, the project also carried out nontechnical tasks, including stakeholder engagements, technology-transfer activities, and project-benefits evaluations. These efforts are summarized in Chapter 4: Conclusion.

Task 9: Evaluation of Project Benefits

This task involved gathering feedback over the project's life using benefit questionnaires, with completion of initial, mid-term, and final questionnaires focused on the project's impact areas

and updates. The final questionnaire summarized the project's key benefits, which include an improvement over traditional manual inspections as well as the provision of real-time data on strain, temperature, and acoustics.

Like the initial and the mid-term assessments, the final questionnaire highlighted the feasibility of DFOS technology for use by FOSW developers. The project has achieved laboratory validation and pilot-scale field testing, marking significant progress toward operational deployment. The final evaluation determined the project's contributions to California's renewable energy mandates and their promising role in enhancing structural monitoring of OWTs through advanced fiber-optic sensing systems.

Project Partners and Participants

The success of the project relied on collaboration with key stakeholders who provided expertise, facilities, and technical support. Major project partners follow.

- **University of California, Berkeley:** Provided access to laboratory facilities, including a shake table used for simulating dynamic loads on wind towers. The university also supported data analysis and interpretation, ensuring that the experimental conditions closely replicated those identified in offshore environments.
- **Siemens Gamesa:** Supplied modern gearbox models and expertise in gearbox monitoring, which were crucial for the operational monitoring experiments. Its involvement ensured that experiments aligned with industry standards and practices.
- **Monterey Bay Aquarium Research Institute:** Collaborated in marine mammal detection studies by providing access to hydrophone data and supporting the deployment of DAS systems in Monterey Bay.
- **National Renewable Energy Laboratory (NREL):** Provided an operating wind turbine at its National Wind Technology Center for the testing of DFAS for the operation of the gearbox under realistic field conditions, which provided key datasets to compare with the bench tests conducted at Siemens Gamesa.

Key Project Milestones

Several key milestones were achieved throughout the project, each contributing to the overall success of the research:

- **Validation of Optical Sensing Technologies:** Successfully demonstrated the feasibility of ϕ -OTDR (ϕ -optical time domain reflectometry) and OFDR for monitoring wind tower strain, providing critical insights into structural health monitoring of OWTs.
- **Real-Time Gearbox Monitoring:** Developed a reliable methodology for real-time monitoring of gearbox performance, offering the potential to reduce maintenance costs and enhance the operational lifespans of wind turbines.

- **Environmental Impact Assessment:** Established the viability of DAS as a tool for monitoring marine life around FOSW installations, addressing key environmental concerns associated with offshore wind energy development.

Summary

To summarize, the project was structured so that each task builds on the previous task, creating a cohesive flow from initial evaluation to real-world field demonstration.

Task 1: Initial Technological Evaluation established foundational knowledge of the critical OWT issues and focused on the potential for DFOS to enhance monitoring of turbine components and environmental impacts. This task provided the baseline technological understanding needed for the project experiment setups and the facilities required for testing.

Task 2: Development of an Advanced Laboratory Testing Facility leveraged the initial technological evaluation to design a facility for rigorous testing. The facility allowed for simulation of realistic static and dynamic conditions where DFOS was tested for real-time monitoring capabilities. This enabled an accurate evaluation of DFOS's performance in structural health monitoring and provided critical data for future tasks.

Task 3: Laboratory Studies to Validate Technology Feasibility advanced the facility capabilities forward using large-scale laboratory tests to validate DFOS technology's effectiveness in detecting strain and temperature changes in wind turbines in real-world conditions. The controlled experiments also helped refine installation techniques, setting the stage for further development in Task 4 and Task 5.

Task 4: Developing Numerical Capabilities for Data Collection, Processing, Analysis, and Visualization focused on data management from the previous tasks' experiments. This involved developing advanced numerical tools to process large datasets, which allowed for real-time and high-precision monitoring of wind turbines and marine environments. These tools were crucial for the data analysis in controlled failure experiments (Task 5).

Task 5: Controlled Failure Experiments and Associated FOS Signals built directly on Task 3 by conducting failure mode experiments to test DFOS's ability to detect bolt loosening and structural anomalies. These experiments simulated real-world damage scenarios to refine predictive maintenance techniques.

Task 6: Numerical Approach Improvements Based on Failure Mode Experiments applied the results from Task 5 to improve data processing and detection methods for wind turbine integrity and marine mammal monitoring. The work emphasized refining frequency mode analysis and noise filtering, directly benefiting subsequent field tests.

Task 7: Field Test Planning and Preparation used the insights from previous laboratory and failure experiments to prepare for real-world testing. This stage involved simulating operational conditions and field testing in partnership with industry leaders, including Siemens Gamesa.

Task 8: Field Demonstration then tested the technologies in actual or simulated offshore environments, testing DFOS and DAS in real-world operational contexts. The success of this

task demonstrated the project's progress toward the practical, operational deployment of these monitoring technologies.

Task 9: Evaluation of Project Benefits consolidated feedback from the entire project lifecycle, assessing its renewable energy goals and improvements in the structural monitoring of OWTs. Each task, in succession, built a deeper understanding of DFOS technologies, culminating in their validation and readiness for real-world applications.

CHAPTER 3:

Results

This chapter summarizes key results from the main experiments conducted during the project that focused on (1) wind tower monitoring; (2) gearbox operation monitoring; and (3) marine mammal detection, in Monterey Bay.

Wind Tower Monitoring

This experiment used an older, full-scale Nordtank 65-kW turbine, with a scale large enough that any limitations in the spatial resolution of ϕ -OTDR could be evaluated. The turbine was not too large to test at the shake table laboratory at the University of California, Berkeley Pacific Earthquake Engineering Research Center facility. Dynamic strain profiles of the magnitudes and frequencies expected for new floating offshore turbines were simulated using the shake table. Importantly, the older full-scale turbine still possessed important characteristics (geometry, connections) required to evaluate monitoring challenges and limitations.

Technologies Used

The OFDR data was collected using a commercial system (Luna Innovation Inc., 2018). This commercial system had strain rate measurement limitations. When the strain rate was high, either temporally or spatially, the readings at those locations became unreliable, limiting the accuracy of dynamic strain profiles.

The ϕ -OTDR technology was also used to measure the optical-phase change. The ϕ -OTDR data was collected using an OptaSense ODH4 interrogator. During the 4-point bend test, a sampling rate of 1 hertz (Hz), with a gauge length of 2 meters and a readout spacing of 1 meter was used. During the shake table test, a sampling rate of 4 kilohertz (kHz) was used to record strain. The phase change measurement was then converted to a mechanical strain measurement using a scaling factor (Grattan, 2000; SEAFOM, 2018).

The 4-point bend test and shake table test were conducted to compare the performance of ϕ -OTDR to OFDR for static strain and dynamic strain, respectively. For both tests, different bolts were loosened to determine if the fiber-optic technologies could detect the change induced by the bolt loosening in the local and global strain fields.

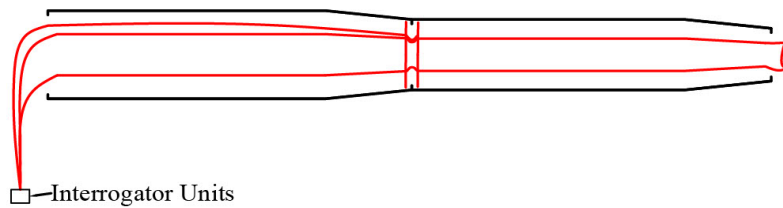
Four-Point Bend Test

The fiber-optic cables were oriented longitudinally along the tower's height, and circumferentially just above and below the flange connections. The layout of the cables for the 4-point bend and shake table tests are shown in Figure 1 and Figure 4, respectively.

To compare the performance of ϕ -OTDR and OFDR under a quasi-static load test, a 4-point bend test was conducted. The bottom two sections were connected in the fully bolted configuration, then supported by two cranes to provide a simply supported beam

configuration. The tower segment was then loaded at two locations. The load was provided by weights that were loaded onto two pallets. Lead weights weighing 500 pound force (lbf) were placed onto each pallet, one at a time, as shown in Figure 1 and Figure 2. Weights totaling 4,000 lbf (2,000 lbf on each pallet) were added. After placing the weights on the pallets, dynamic vibrations were allowed to decay. A single 500-lbf weight was then removed from each pallet, resulting in a total of 3,000 lbf. This process was repeated until the pallets had no lead weights. The loading configurations are summarized in Table 1. Measurements were taken throughout the duration of the bend test, with no interruptions.

Figure 1: Fiber-Optic Installation Layout (in Red) for the 4-Point Bend Test (Side View)



Source: LBNL

Figure 2: Turbine Being Loaded With Weights During the 4-Point Bend Test



Source: LBNL

Table 1: Four-Point Bend Test Loading Configurations Used for Each Bolt Configuration

Loading Configuration	Total Weight
1	4,000 lbf (17,793 N)
2	3,000 lbf (13,345 N)
3	2,000 lbf (8,896 N)
4	1,000 lbf (4,448 N)
5	0 lbf (0 N)

N=newtons
Source: LBNL

Shake Table Test

In the shake table test, the full turbine tower was subjected to ground motions that induced typical dynamic strain profiles experienced by OWTs. Appropriate ground motions were selected using the open-source computational tools OpenSees and OpenFAST. OpenSees, a finite element modeling framework originally developed for earthquake engineering, modeled and simulated the Nordtank wind turbine under shake-table motions. This confirmed that the expected dynamic strain profiles were similar to those from the prototype model (simulated using OpenFAST). The Nordtank turbine tower was modeled with 50 beam-column elements: 10 elements each for the non-tapered and tapered sections. Properties such as flexural stiffness and weight were assigned based on the cross-section at each element's midpoint.

All three tower segments and the nacelle, with added weight, were assembled onto the base plate and placed on the shake table (Figure 3). Based on OpenFAST simulations of the prototype FOWT and OpenSees simulations of the Nordtank tower, the desired strain frequencies were around 0.5 Hz for wave loading and near static (0.05 Hz) for wind loading. Due to the shake table's limited stroke, simulating motion at 0.05 Hz was impractical. To address this, an additional 2,000 lbf (8,896 N) weight was placed in the nacelle about 2 meters off-center to represent steady wind loading, and the turbine was tilted southward to induce extra static load. The tower was subjected to three loading configurations, summarized in Table 2: (1) sinusoidal horizontal ground acceleration at 0.5 Hz with a 4.8-inch amplitude, (2) the same acceleration with a 0.8-degree tilt southward, and (3) sinusoidal rotation about the base with a 0.8-degree amplitude at 0.5 Hz. All loading configurations were repeated for each bolt configuration.

Figure 3: View of Wind Turbine on the Shake Table, From the Base



Source: LBNL

Figure 4: Fiber-Optic Installation Layout (in Red) for the Shake Table Test (Side View)

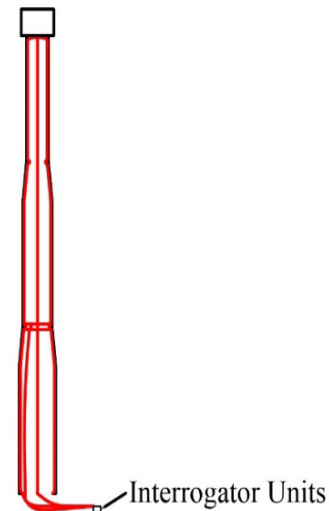


Table 2: Shake Table Test Loading Configurations Used for Each Bolt Configuration

Loading Configuration	Loading Description	Frequency	Amplitude
1	North-south translational sinusoidal shaking	0.5 Hz	4.8 inches
2	North-south translational sinusoidal shaking with tilt	0.5 Hz	4.8 inches
3	North-south rotational sinusoidal shaking	0.5 Hz	0.8 degrees

Key Technical Barriers

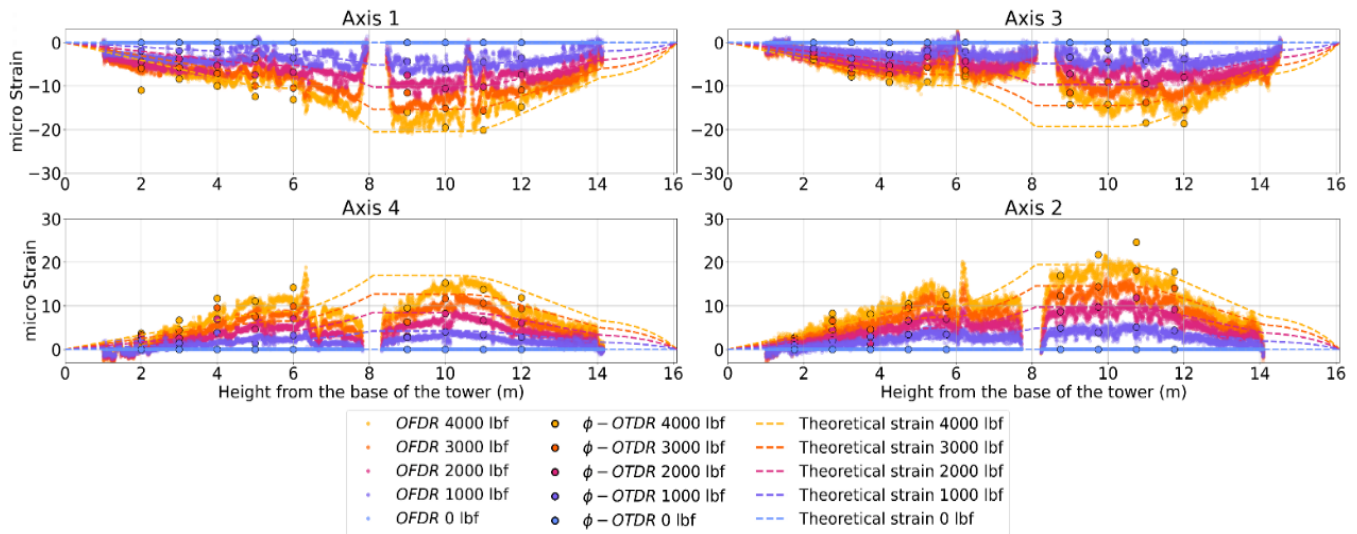
Monitoring floating OWTs is technically challenging because their large and dynamic loads exceed the traditional targets seen in infrastructures like bridges and buildings. Validating the ability of DFOS technologies (like ϕ -OTDR) to measure static and dynamic strain in these turbines is essential and should be comparable to industry-accepted OFDR systems. Assessing the data quality from ϕ -OTDR is crucial to ensure that frequency information of the system response is preserved. This experiment also explored the mechanical effect of bolt loosening on the local strain field. To address these challenges, controlled tests were conducted to validate ϕ -OTDR technology under both static and dynamic loads using wind-turbine towers; results were then compared with OFDR technology in lab experiments. This comparative data is discussed in the following section.

Key Results

Ability to Identify Strain Profiles With 4-Point Bend Tests and Integrity Issues

Figure 5 compares ϕ -OTDR and OFDR measurements of the strain under all load configurations for a particular bolt configuration. The measurements were zeroed with respect to the final loading configuration of 0 lbf of their respective bolt configuration. Figure 5 also shows the theoretical strain, assuming simply supported boundary conditions, Euler-Bernoulli beam theory assumptions, and a simple tube cross-section with various diameters, but it ignores the complexities of the flange connection. The ϕ -OTDR and OFDR measurements are generally in good agreement. Figure 5 shows that the measurements have the same shape as the expected bending strain distribution. While Axis 1 and Axis 2 are similar in shape and magnitude, Axis 3 and Axis 4 show sharp decreases in magnitude near the flange connection. These decreases in axial strain may be due to the fiber-optic cables associated with Axis 3 and Axis 4 alignment with the stiffeners, resulting in a greater local bending stiffness. The ϕ -OTDR and OFDR measurements were in good agreement, which may indicate that it is the true strain.

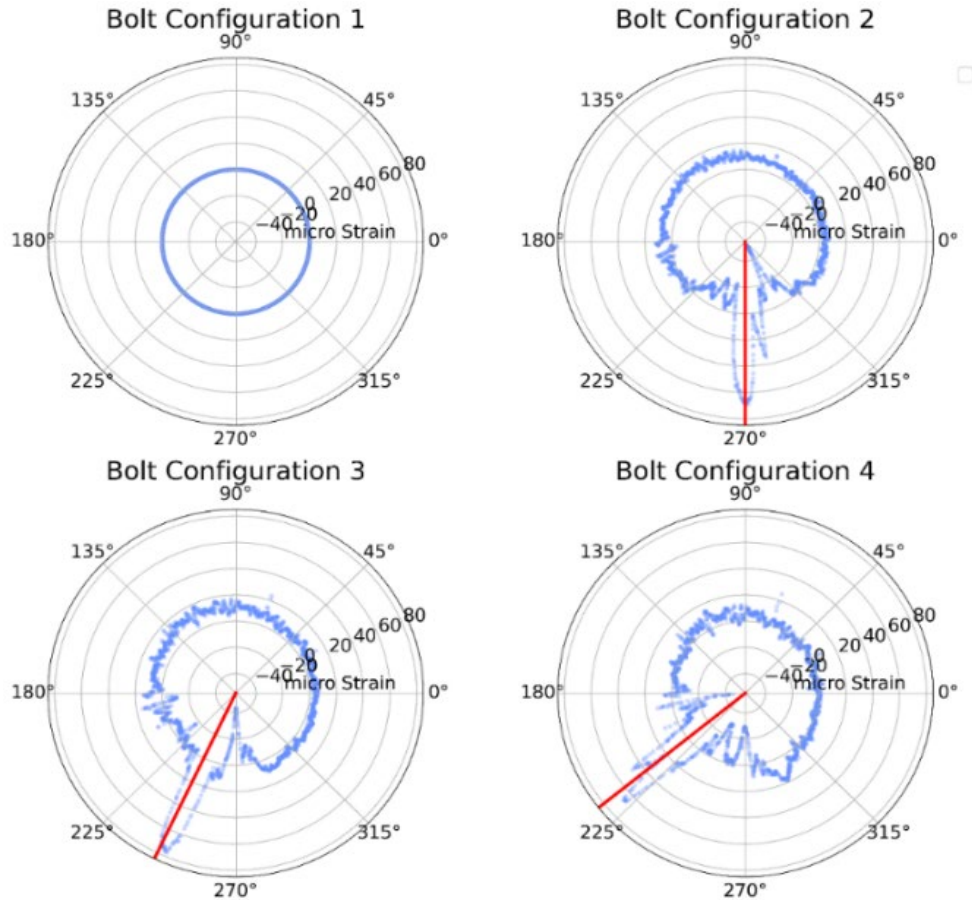
Figure 5: Axial Strain for Bolt Configuration 1, With Theoretical Strains Plotted



Source: LBNL

Due to ϕ -OTDR's phase-determination errors, which were especially problematic with step-like loading as in the 4-point bend test, comparing different bolt configurations was difficult. In contrast, OFDR did not suffer from these errors and allowed for such comparisons. Figure 6 shows OFDR strain profiles across all bolt configurations at 0 lbf load, zeroed relative to Bolt Configuration 1 (hence, it appears at 0 microstrain). In subsequent configurations, there was a significant increase in hoop strain at the locations of the loosened bolts — even under the turbine's self-weight — before the application of additional weights. This demonstrated that fiber optics can detect changes in the local strain field due to bolt loosening, proving its potential for monitoring joint-integrity issues.

Figure 6: Circumferential Strain for All Bolt Configurations

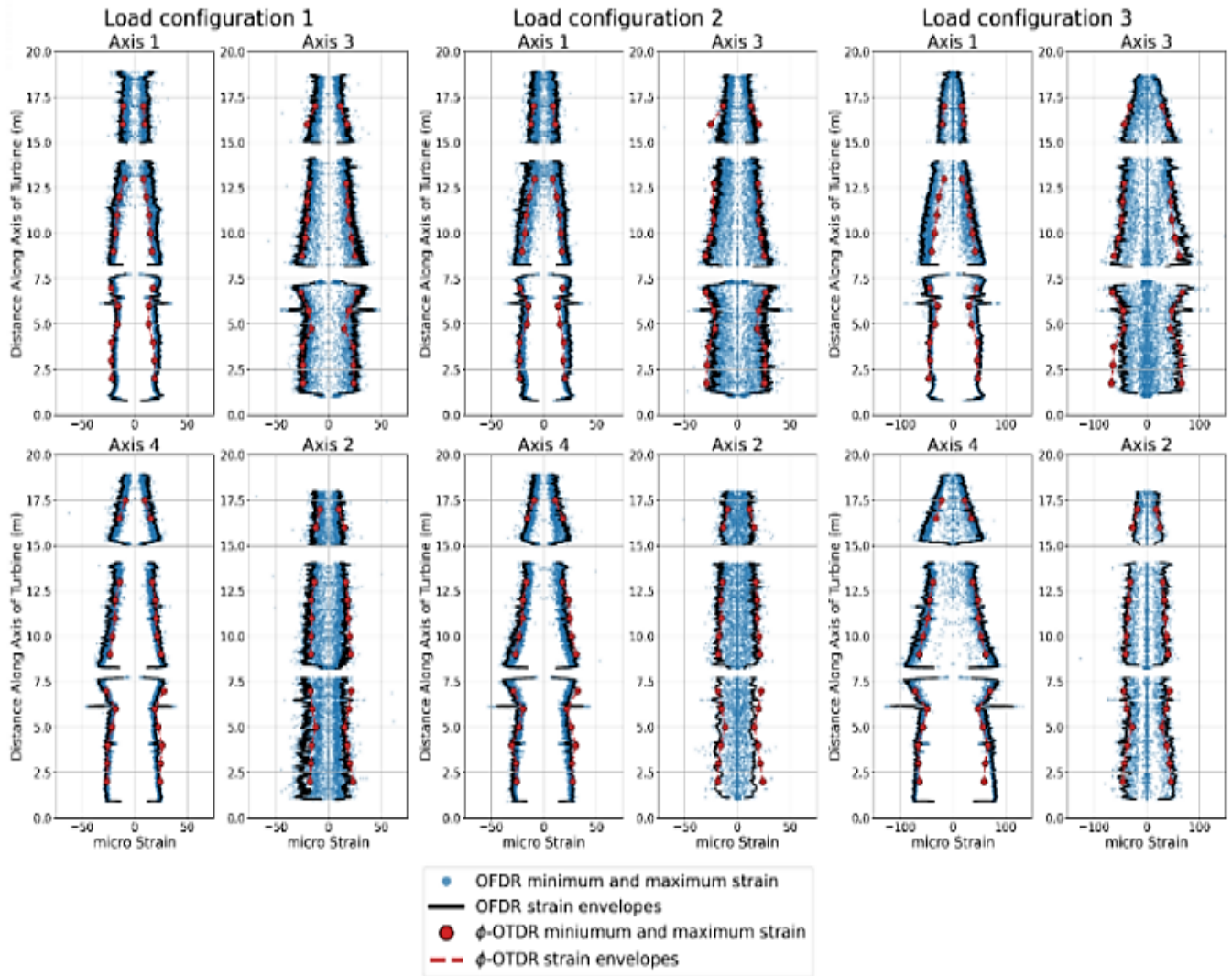


Source: LBNL

Strain Analysis and Frequency Response During Shaking

During the shake table test, OFDR experienced severe signal loss due to the high strain rate environment during the duration of shaking. Due to signal loss of OFDR, a comparison between the maximum and the minimum strains measured by OFDR and ϕ -OTDR was made. The comparison of the minimum and the maximum strain envelopes for Bolt Configuration 1 is shown in Figure 7. Good agreement between the strain envelope profiles was observed when compared with ϕ -OTDR profiles matching the OFDR profiles.

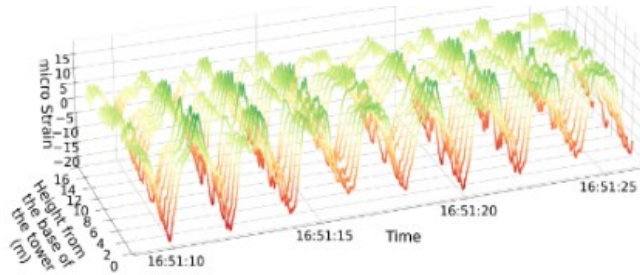
Figure 7: Strain Envelope Comparisons for Bolt Configuration 1



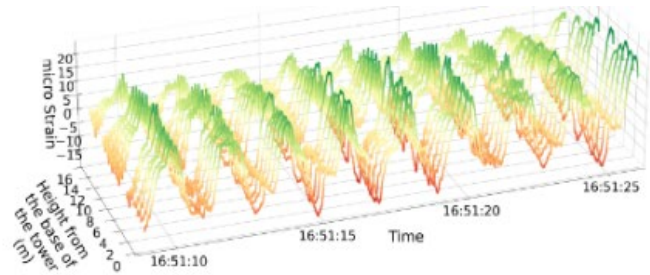
Source: LBNL

Figure 8 shows the strain time series measured by ϕ -OTDR. The response of the two south axes (Axis 2 and Axis 3) and the response of the two north axes (Axis 1 and Axis 4) have similar amplitudes and are 180 degrees out of phase (i.e., when the south axes experience a tensile [positive] strain, the north axes experience a similar magnitude compressive [negative] strain), as expected.

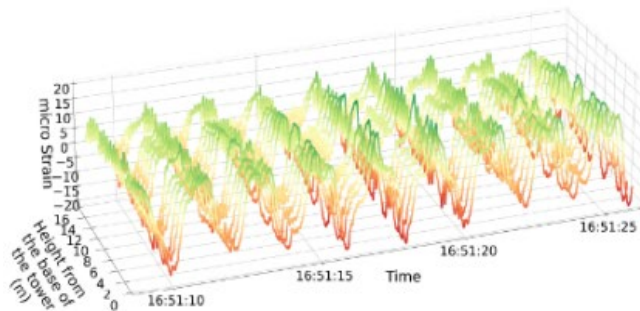
Figure 8: ϕ -OTDR Strain Time Series During the Translational Loading Configuration for Bolt Configuration 1



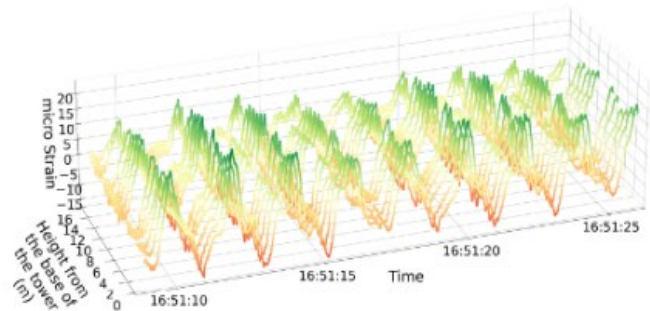
(a) Axis 1.



(b) Axis 3.



(c) Axis 4.



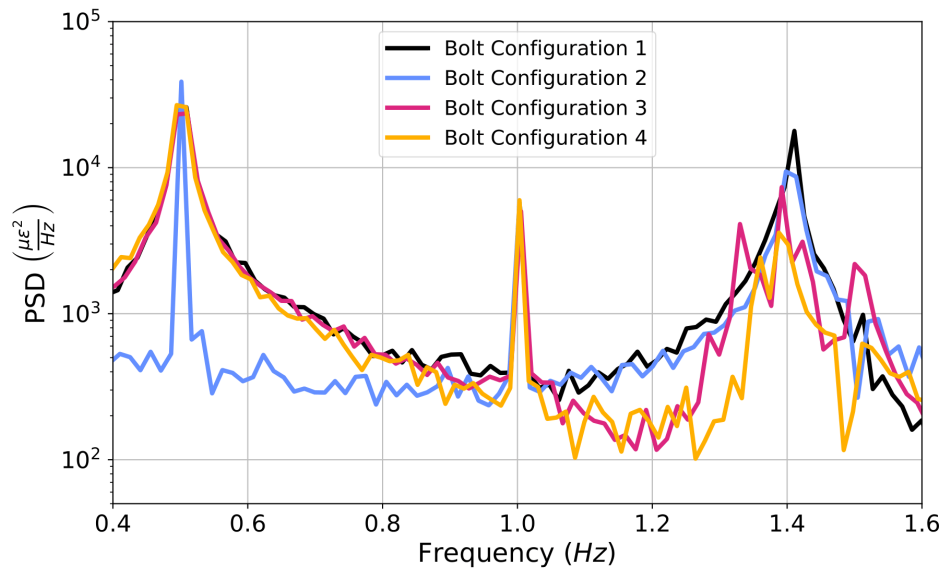
(d) Axis 2.

m=meters

Source: LBNL

Figure 9 shows the averaged power spectral densities of all the sensors in the bottom section of Axis 3 of the ϕ -OTDR sensors during translational shaking at 0.5 Hz. The power spectral densities were calculated after applying a high-pass filter with a cutoff frequency of 0.15 Hz. The forcing frequency at 0.5 Hz was clearly identified, and there were peaks at integer multiples of 0.5 Hz (harmonics) due to shake-table loading. There was also a peak that corresponded with the natural frequency of the turbine, occurring around 1.4 Hz. The natural frequencies of the bolt configurations are identified in Table 3.

Figure 9: Averaged PSD Values for Longitudinal Channels in the Bottom Section of Axis 3 Using Φ -OTDR Data During Translational Shaking (With Tilt)



PSD=power spectral density; $\mu\epsilon^2/\text{Hz}$ =square microstrains per hertz

Table 3: Shake Test Averaged PSDs For Each Bolt Configuration During Loading Configuration 2

Bolt Configuration	Identified Natural Frequency (Hz)
1	1.411
2	1.398
3	1.392
4	1.388

Source: LBNL

Summary

In this experiment, a Nordtank 65 kW turbine was used to assess the technical feasibility and performance of DFOS technologies, specifically ϕ -OTDR and OFDR, for real-time strain monitoring of FOWTs. A 4-point bend test and dynamic shake table test simulated strain profiles, with ϕ -OTDR showing reliable detection of both static and dynamic strains despite OFDR's experiencing signal loss under high-strain rates. The ϕ -OTDR effectively detected strain variations caused by bolt loosening, and power spectral-density analyses highlighted the turbine's natural frequency at approximately 1.4 Hz, aligning with theoretical predictions. This study validated the potential for using DFOS for monitoring strain profiles and structural integrity for FOSW applications.

Gearbox Operation Monitoring

Gearbox malfunction is the most frequent cause of wind turbine failure. Real-time monitoring is critical for detecting prefailure warning signs, but current point-based sensors offer limited spatial coverage and can't pinpoint small anomalies on large gearboxes. To overcome this, the research team focused on planetary stages with stationary ring gears. The forces transferred to the ring gear and measured by DFOS were proportional to the external torque input, and they were equally distributed to the planet gears that mesh with the ring gear's interior teeth. Because ring gears are relatively thin, significant deformations were observed on their outer surfaces where optical fibers were installed. By monitoring strain on the ring gear, torque can be measured to detect operational abnormalities. Since testing DFOS technologies on operational FOWTs wasn't feasible, the team conducted tests on a standalone modern gearbox in collaboration with Siemens Gamesa and on an experimental wind turbine at the NREL National Wind Technology Center.

Experimental Setup

The tested gearbox featured two planetary stages and one helical stage. The first planetary stage contained four planet gears housed by planet carriers, acting as the input or low-speed shafts. When the motor rotates, these planets mesh simultaneously with the ring gear, with gear mesh forces proportional to the input carrier torque. These forces are transmitted through multiple teeth via contact lines between the planet gears and the ring gear, causing significant strain on the ring gear. A sensing fiber was attached to the outer surface of the ring gear of the first planetary stage, for measurements. Operating parameters like torque inputs were recorded to support DFOS data analyses. An identical sensor setup was used for both bench-scale testing at Siemens and field-testing at the NREL National Wind Technology Center.

Key Technical Barriers

The primary challenges in this study were to accurately measure the strain on the gearbox during operation (using strain readings to predict the condition of the gearbox), including torque input of the wind turbine, and to detect potential gearbox failures. These tasks were complicated by the rotational motion of the gears, temperature variations, and potential interference from the optical fiber installation process.

Solutions to the Barriers

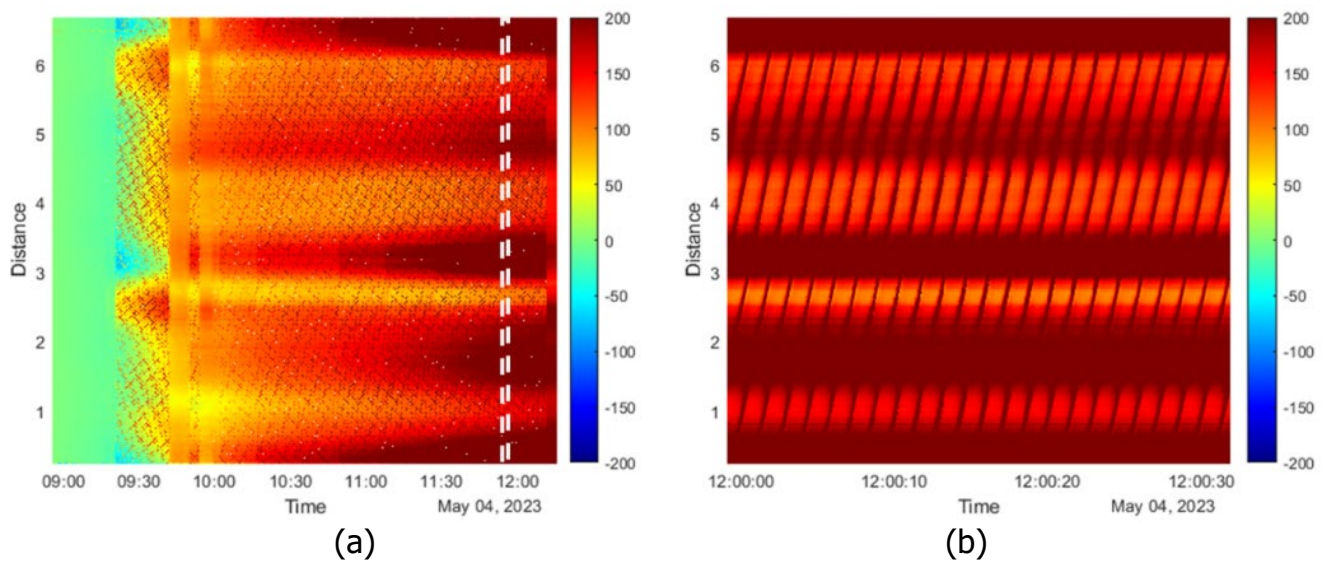
To address these challenges, a DFOS system with high spatial resolution and strain-measurement accuracy was used. A high-pass filter was applied to mitigate temperature effects, and the optical fiber was installed to minimize polarization fading and micro-bending. This setup and data analysis method allowed real-time monitoring of the gearbox's performance and torque input predictions.

Key Results

Strain Profile Analysis and Data Visualization

For accurate strain monitoring, the data obtained needed to be calibrated to remove the temperature effects that impacted the fiber. Waterfall plots of time versus distributed signals were used to visualize the movement of the planetary gears. The raw strain recordings, shown in Figure 10a, indicate tension (red) and compression (blue) in the gears. A detailed 30-second interval (Figure 10b) highlights the rotation direction of the four planet gears. As the test progressed, a shift towards red indicated a temperature rise due to frictional heat generated by gear movement.

Figure 10: Waterfall Representation of the Strain Profile Over Time for the Circumference of the Ring Rear

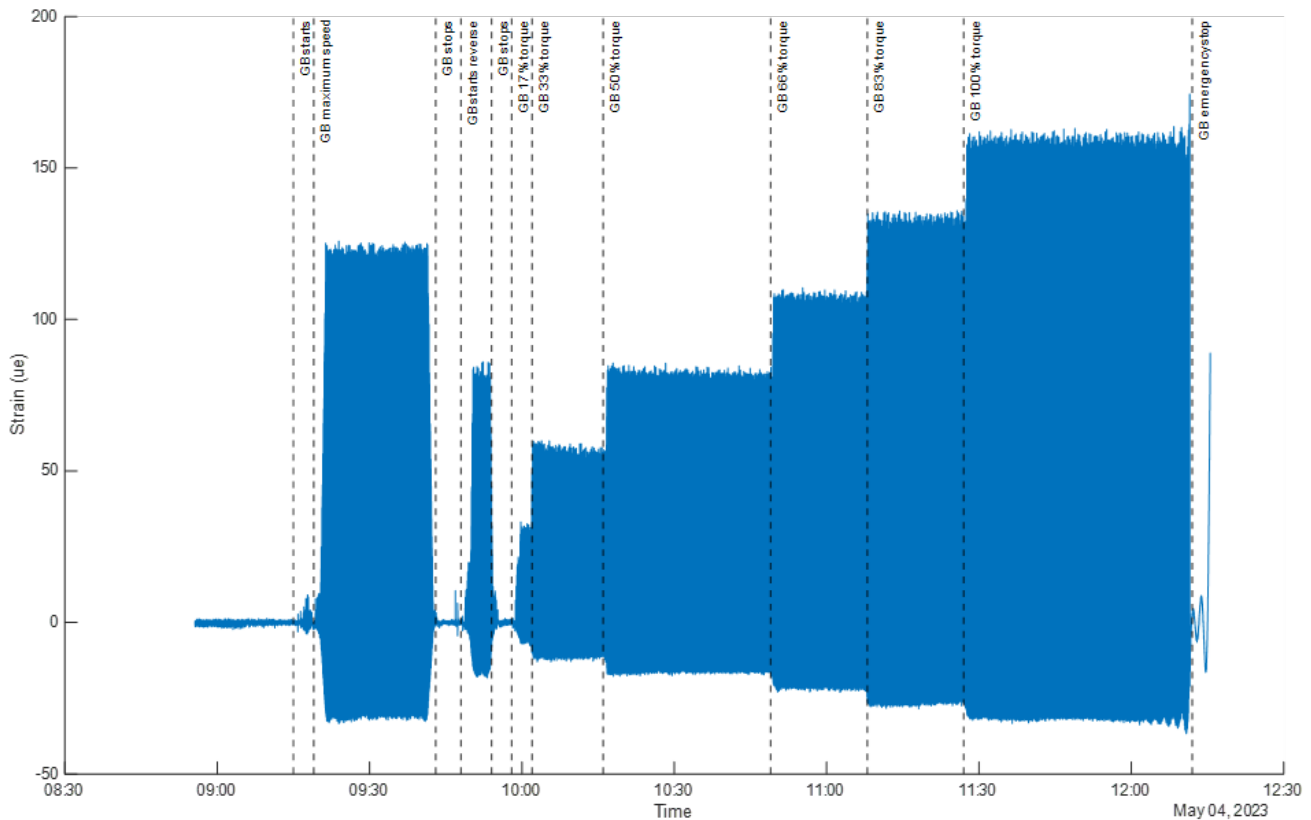


The vertical axis represents distance in meters, while the color gradient indicates strain in micro-strain. (a) A strain profile throughout the entire test period, and (b) a magnified view of the strain profile corresponding to the region outlined by the white-dashed square in the left panel.

Source: LBNL

After the application of a 0.01-Hz high-pass filter, the strain profiles at maximum load showed a twill-like pattern reflecting planet gear rotation. This suggested that five ring gear teeth were in contact during rotation, with the highest load on the middle two teeth, likely due to the gear teeth's helix angle and strain during engagement. This analysis demonstrated that each tooth's strain response can be monitored during operation. Figure 11 shows the strain response to torque changes, indicating the sensitivity of strain measurements to torque.

Figure 11: Strain Response After 0.01-Hz High-pass at Location 4.62 M

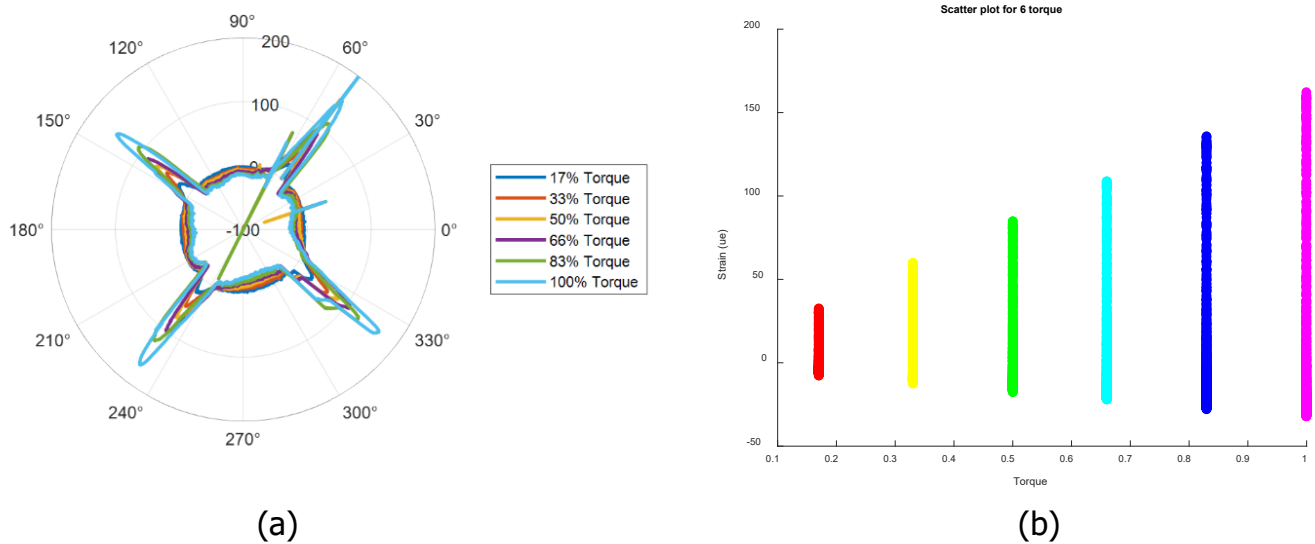


The dashed line shows the timing of each loading event listed in Table 2.

$\mu\epsilon$ =microstrains
Source: LBNL

Using a polar axis representation, strain profiles at various loads were visualized to demonstrate DFOS's real-time monitoring capabilities (Figure 12a). The four ramps in the plot represent the strain values from the four planet gears as they rotated in sync with gear movement. Six strain profiles at different torque inputs were plotted when the gears were in similar positions. As the load increased, tension strain escalated at contact points with the planet gears, while compression increased between them. Figure 12b highlights these changes at a single location across all load levels, including when the gear both engages and disengages.

Figure 12: Strain Profile in Polar Axis and the Strain Versus Torque Input



(a) The strain profile in polar axis when different loads were applied to the gearbox, and (b) the scatter plot of all the collected strain at one location on the ring gears during the load test with different load input

Source: LBNL

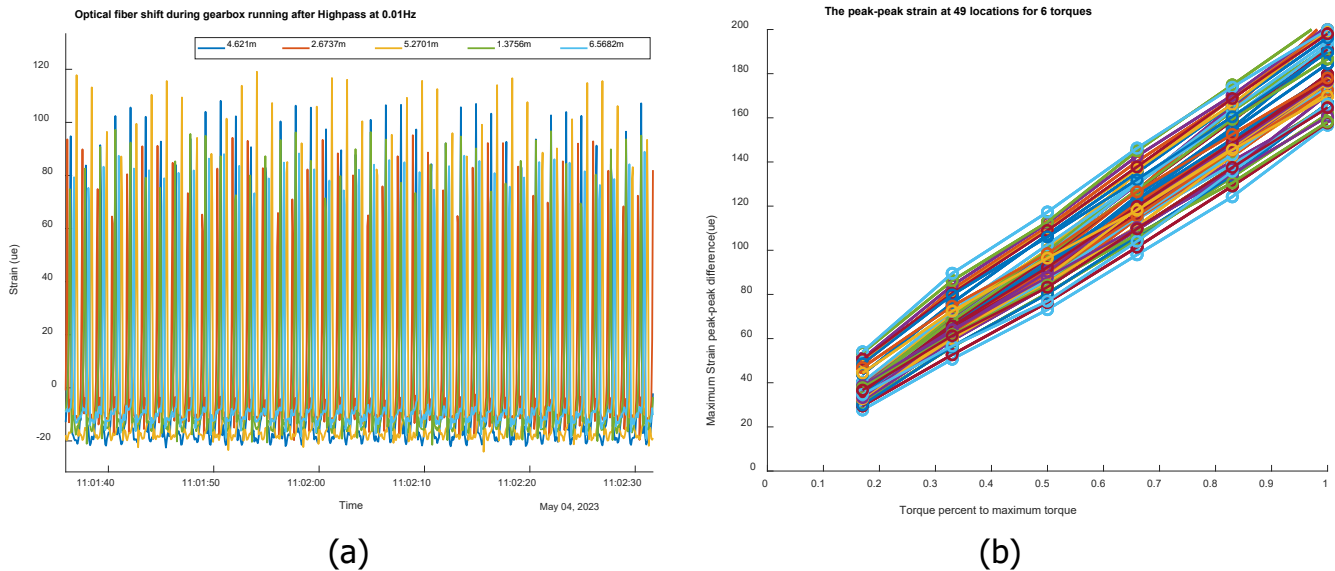
Quantification of Gearbox Metrics

The measured DFOS data quantified gearbox conditions like rotating speed and torque. Strain variations at five specific locations showed distinct spikes corresponding to the rotation of the planet gears (Figure 13a). Each spike represents the arrival and departure of a planet gear, with intervals of 1.44 seconds, equating to a rotational speed of 5.76 seconds per rotation (or 10.42 revolutions per minute [rpm]). A periodic signal of six spikes over 8.64 seconds was also observed, possibly due to variations in motor-input torque.

Calculating peak-to-peak strain at 49 locations revealed a strong linear relationship between load and strain, with an R^2 of 0.9997 (Figure 13b). This confirmed the operational health of the gearbox and suggests that torque input can be accurately predicted from strain measurements.

The gearbox was new and in pristine condition, which likely contributed to the strong linearity between load and strain. As the gearbox ages or encounters issues, deviations from this linearity may occur at certain locations. Therefore, fault detection can be performed by monitoring these deviations and examining linearity across all gearbox locations.

Figure 13: Strain Reading at Different Locations Versus Time and Torque Inputs



(a) An example of collected strain at 5 locations with time, and (b) the peak-to-peak strain at 49 locations on the ring gear for 6 torque load inputs.

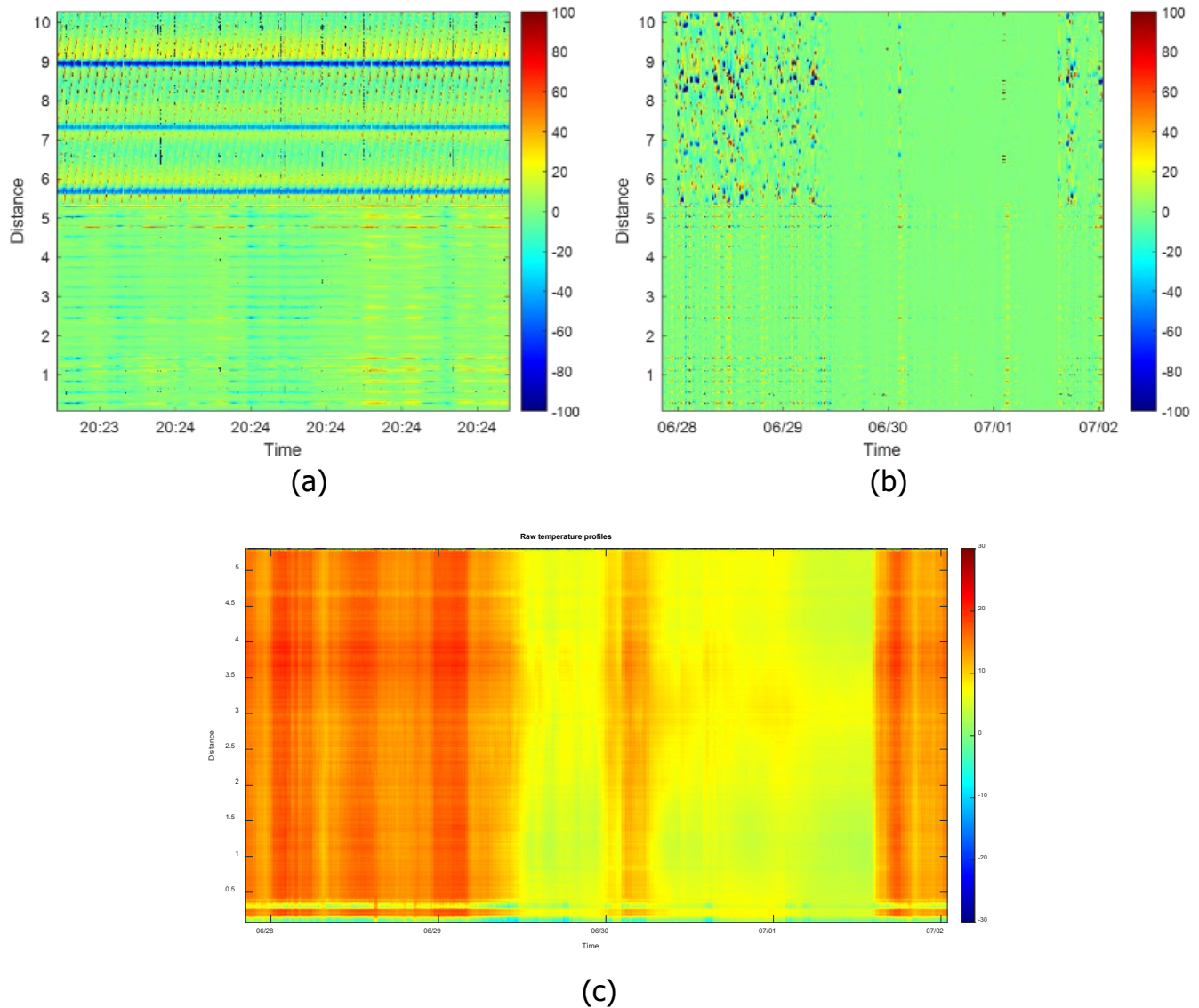
Source: LBNL

Real-Time Validation in Operational Wind Turbine

The method was tested on a GE 1.5-megawatt wind turbine under real operating conditions at the National Wind Technology Center in Flatiron, Colorado. The DFOS was installed on the outer surface of the ring gear, as with the bench test, and data were compared with the turbine's power output and torque measurements.

Figure 14 shows strain readings after applying a 12.5-Hz high-pass filter, along with temperature measurements. On June 29, 2022, and July 1, 2023, the turbine was shut down for several hours. Strain readings along the ring gear (from 5.4 to 10.2 meters) fluctuated with the turbine's operation. Temperature increased by about 10 degrees during power generation, indicating stronger power output (darker red regions). A closer look at the strain data (Figure 14a) reveals a pattern caused by the rotation of the three planetary gears; strain values increased (tension) when a planetary gear approached a specific point on the ring gear and decreased (compression) as it moved away.

Figure 14: Strain and Temperature Reading Profiles in the Field Test

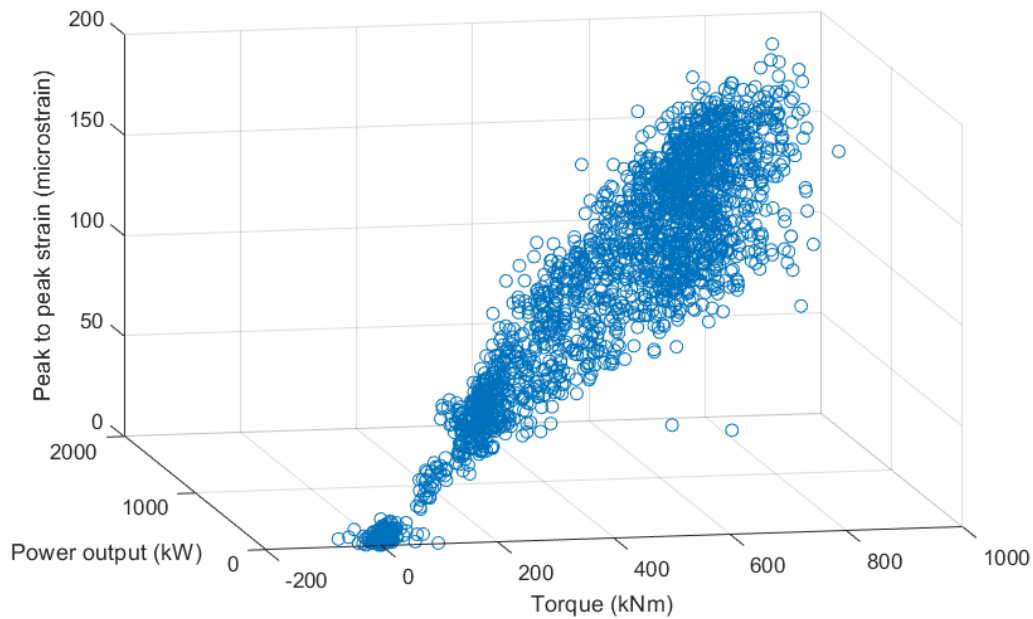


(a) An example strain reading over one minute, (b) a strain reading between June 28 and July 2, and (c) a temperature reading between June 28 and July 2.

Source: LBNL

Figure 15 illustrates the relationship between peak-to-peak strain, input torque, and output power. As the power output increased, the strain (reflecting the tension and compression differences during the planetary gears' rotation) also increased. Variations in strain grew with higher torque and power, although the cause remains unclear and requires further investigation. Compared with the brand-new gearbox for the bench tests, the nonlinearity may (1) result from material behavior changes after service for more than 10 years, or (2) could be related to the difference in gearbox design. Regardless, the DFOS showed its capability to detect the condition of the gearbox, although there are still questions to be answered to link the strain response to the structural strength of the ring gear and the efficiency of load transfer between the ring and planetary gears.

Figure 15: Peak-to-peak Strain With Input Torque and Output Power in the Field Test



kNm=kilonewton meters
Source: LBNL

Summary

Experiments using DFOS for gearbox monitoring demonstrated high sensitivity and accuracy, providing crucial data for prefailure diagnostics that support proactive maintenance. Utilizing OFDR technology, DFOS offers millimeter-scale spatial resolution and approximately 1 microstrain accuracy at a measurement speed of 12.5 Hz. The strain measurements on the first planetary stage confirmed the viability of this application of DFOS technology.

Load tests showed that strain increased linearly with applied torque across all monitored locations. This indicates that DFOS-measured strain can accurately quantify torque, enabling real-time detection of potential gearbox faults by identifying irregular strain before catastrophic failures occur. With high spatial resolution and the ability to track strain on each tooth, DFOS can optimize gearbox design and refine control systems. DFOS is easy to install, and it provides valuable feedback during both design and operational phases, substantially reducing operation and maintenance costs.

Although temperature effects were not deeply explored, this data can also aid in fault prediction through heat detection within the gearbox. These advancements can enhance gearbox design, operation, and maintenance, promoting more reliable and cost-effective wind energy solutions.

Marine Mammal Detection at Monterey Bay

These experiments were conducted at the Monterey Bay National Marine Sanctuary to evaluate the feasibility of using DAS for acoustic monitoring of marine mammals. DAS is a

sensing technology that can repurpose a fiber-optic cable as an array of acoustic sensors. This was the first time DAS was deployed from a boat. The fiber-optic cable was lowered into the water from an A-frame mounted to the stern of the ship to simulate a mooring line installed in open ocean conditions similar to where FOWTs would be deployed. The goal was to deploy DAS as a holistic sensing solution that could both monitor the structural health of FOWT components (Xu et al., 2023; Hubbard et al., 2021) and assess marine life impacts throughout the FOWT lifecycle (Bailey et al., 2010; Madsen et al., 2006). This research focused on the second objective and explored DAS for detecting whale vocalizations.

Experimental Setup

Data acquisition was conducted through three fieldwork expeditions in Monterey Bay, in June 2022, August 2023, and October 2023. During each expedition, the sensing fiber was attached to a mooring line and lowered to depths of between 100 and 400 meters. The DAS interrogator was housed inside the boat cabin.

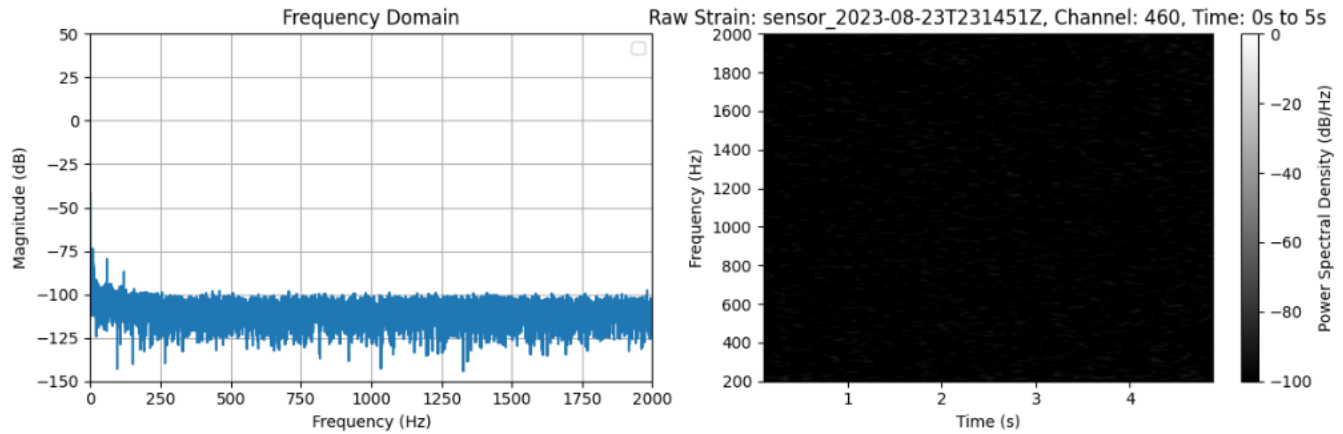
Figure 16: Research Vessel in Monterey Bay With DAS Interrogator Housed Inside the Cabin and DAS Cable Lowered to the Water Using A-Frame



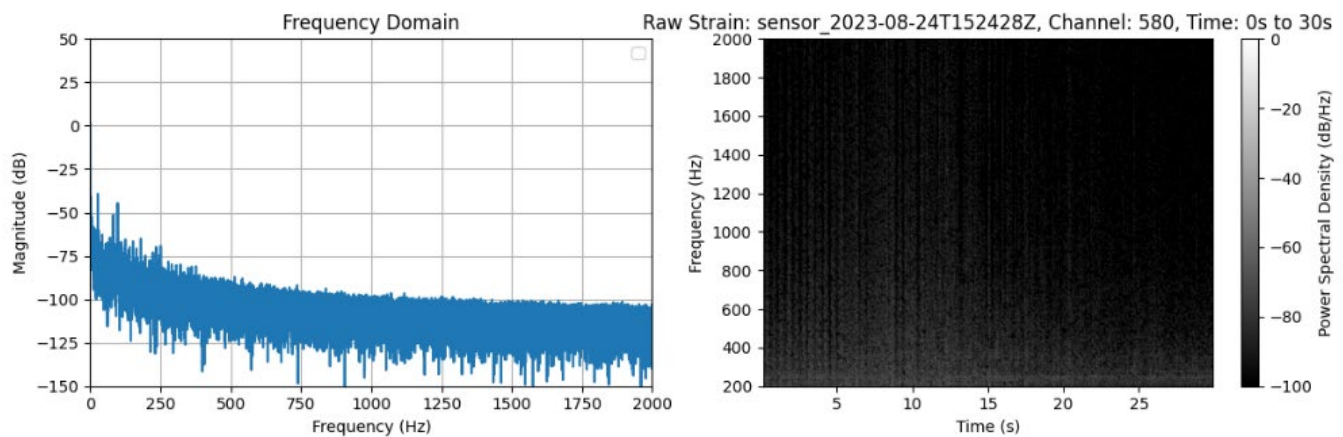
Photo: Jeremy Snyder

Raw DAS data was compared with the boat engine on and off and when the cable was inside a spool or in the water. These comparisons showed the impact of cable placement and surrounding acoustic conditions on DAS data quality (Figure 17). When the boat was stationed at the dock with the engine off and the cable in a spool inside the boat, the noise floor was relatively low (Figure 17, Item 1); the noise floor increased when the boat engine was turned on (Figure 17, Item 2). Once the boat arrived at the destination point, while the engine was on, the cable could still capture the speaker sound when it was in a spool inside the boat. (Figure 17, Item 3). However, once the cable was placed in the water, the speaker sound could no longer be detected (Figure 17, Item 4).

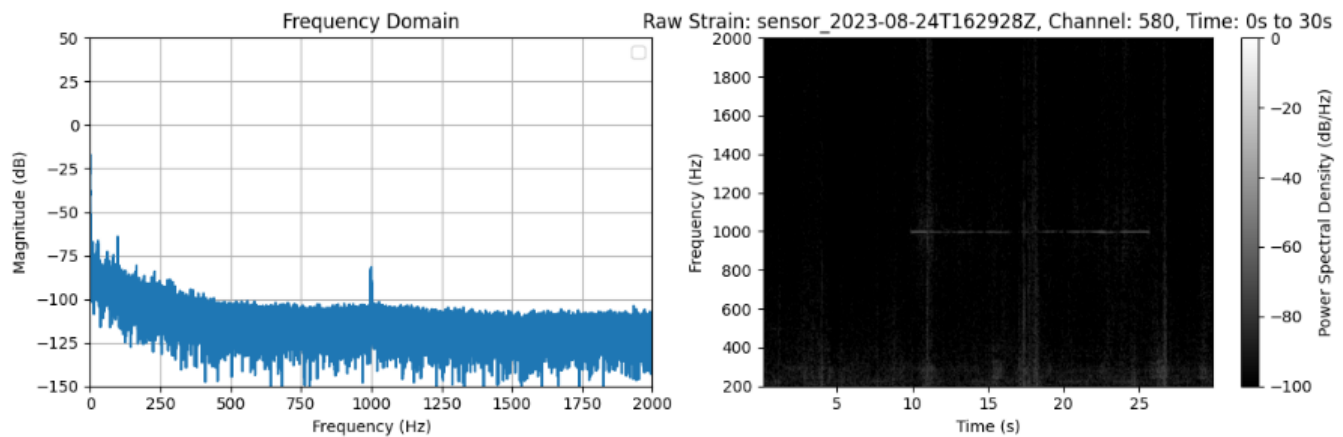
Figure 17: Magnitude Spectra and Spectrograms Compared From Raw DAS Data, Showing the Impacts of Boat Engine Noise and Cable Location on the Noise Floor and the Visibility of Signals



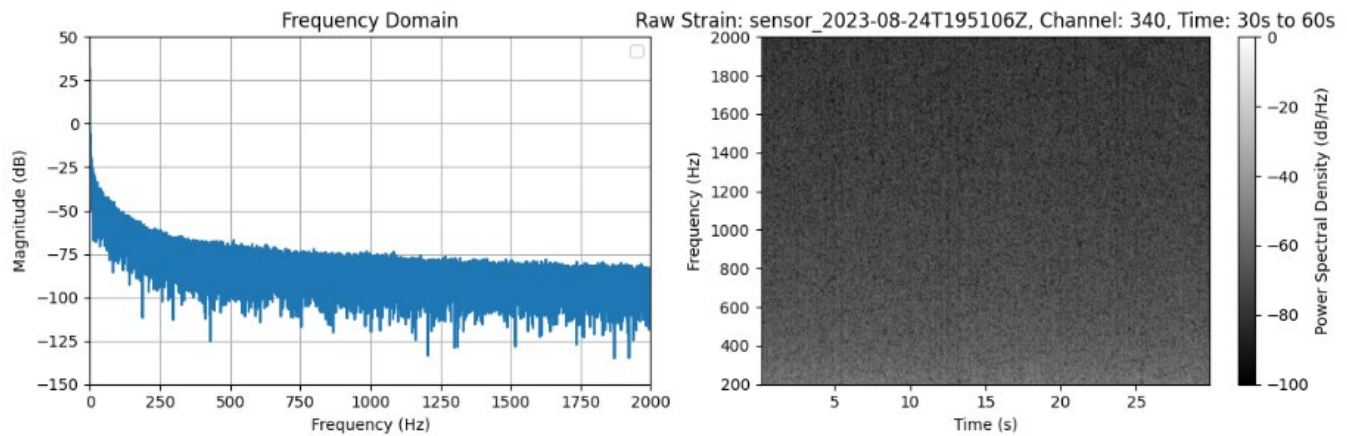
(1) Boat stationed at dock, engine off; cable in spool inside boat.



(2) Boat stationed at dock, engine on; cable in spool inside boat.



(3) Boat at destination point, engine on; cable in spool inside boat; speaking playing 1,000 Hz near cable.



**(4) Boat at destination point, engine on; cable placed in water;
speaker playing 1,000 Hz near cable.**

dB=decibel; dB/Hz=decibels per hertz
Source: LBNL

Throughout the expeditions, data acquisition and experimental setups were revised based on lessons learned from each phase. Different data-acquisition setups, sensing cable types, and cable configurations were tested to improve the stability and positioning of the sensing fiber and to improve the data-collection process.

Key Technical Barriers

Mitigating noise in the DAS recordings was a significant research focus. With the DAS interrogator housed inside the research vessel and the sensing fiber lowered to shallow water depths, multiple sources of noise were present, including engine sounds, wave noise, and the movement and straining of the cable due to wind and water currents. These factors contributed to a complex acoustic environment, which made it challenging to isolate and analyze desired signals.

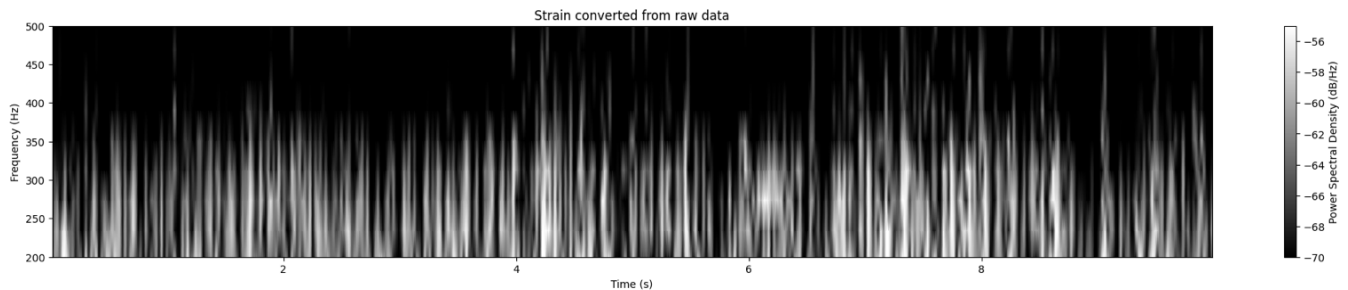
Another major challenge was the uncertainty associated with dynamic noise sources and the occurrence of whale vocalizations. It was difficult to characterize noise, including their types, number, and intensity, when it varied unpredictably over time. This uncertainty was compounded by difficulties in capturing whale vocalizations. Despite visual sightings of whales around the research vessel, it was often unclear when and where the whales vocalized, making it even more challenging to differentiate their calls from surrounding noise sources.

Processing the volume of data collected during these experiments was another challenge. Manual review of this multi-day dataset was time-intensive. The variability in noise levels and signal characteristics required frequent adjustments to spectrogram parameters, since a single set of parameters could not be uniformly applied across the entire dataset due to changes in signal strength, noise interference, and environmental conditions. Figure 18 shows an example of a time series that was adjusted (in terms of spectrogram parameters) to be able to visualize and identify whale vocalizations captured by DAS.

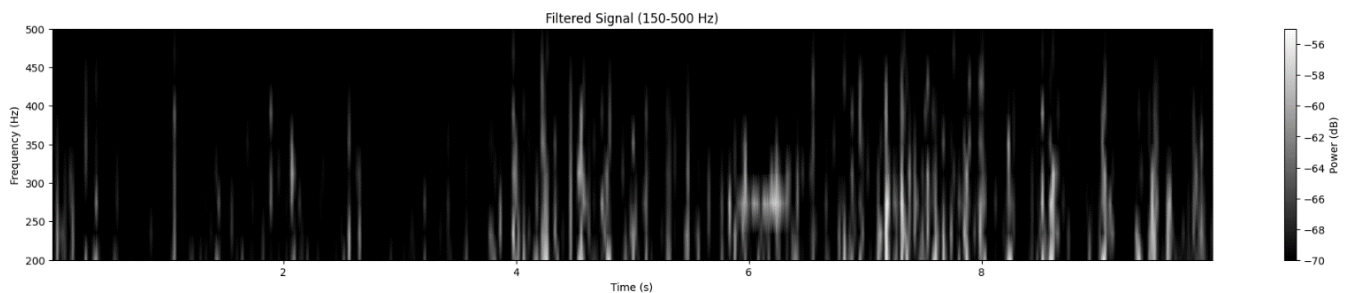
Conventional noise processing and analysis techniques, which are effective for ocean floor DAS deployments (e.g., Wilcock et al., 2023; Bouffaut et al., 2022; Lindsey et al., 2019), do not

suffer from the significant noise and dynamic acoustic sources encountered during testing and were found to be insufficient. This required the development and refinement of new strategies to address these unique and fluctuating noise challenges.

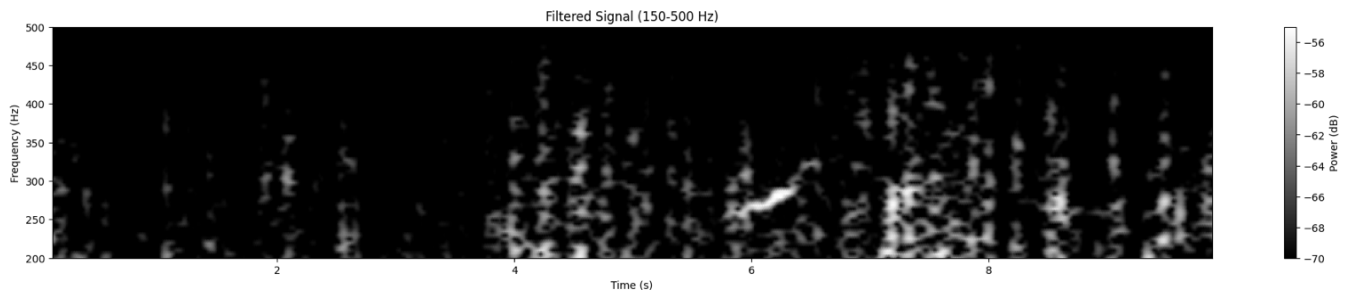
Figure 18: Time Series Adjusted to Visualize Whale Vocalizations – the Signal Recorded at Approximately 6 Seconds Was a Whale Vocalization.



(I) Raw Time Series Without Any Filtering



(II) Time Series After Bandpass Filtering (150-500 Hz)



(III) Bandpass-Filtered Time Series (150-500 Hz) After Adjusting Spectrogram Parameters

Source: LBNL

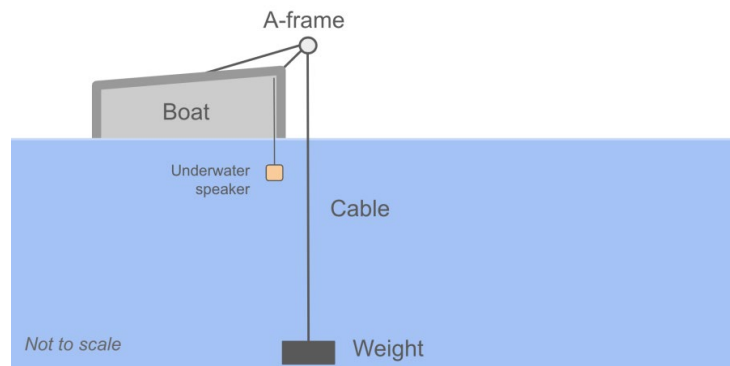
Solution to the Barriers

Solutions were developed to mitigate the impact of noise sources, enhance the quality of the recorded data, and identify whale vocalizations more reliably. The DAS data were examined at different stages of boat operation and with different cable configurations to evaluate their effects on the noise floor. This analysis informed subsequent strategies, including an underwater speaker to generate controlled sounds, adjustments to cable configurations to reduce noise interference, audio-conversion and median-filtering techniques, and cross-

referencing DAS recordings with hydrophone audio to enhance signal clarity. More detail follows.

1. Speaker: An underwater speaker was used to generate controlled acoustic signals, which provided a known sound source. By using the speaker to emit desired frequencies, the DAS system could be tested for sensitivity and accuracy in detecting and distinguishing between various sound sources. To address the uncertainty of real whale vocalizations during data acquisition, a pre-recorded humpback whale song was also played through the speaker. The speaker was placed near the cable (Figure 19).

Figure 19: Schematic of Experimental Setup

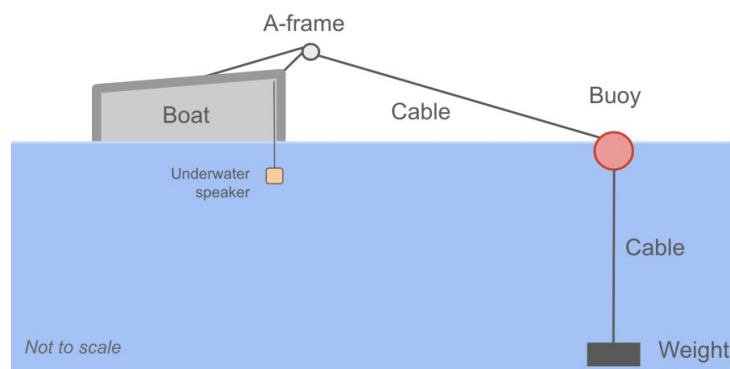


A weight was attached to the end of the DAS cable to maintain a vertical orientation. An underwater speaker was placed near the cable at a shallower depth.

Source: LBNL

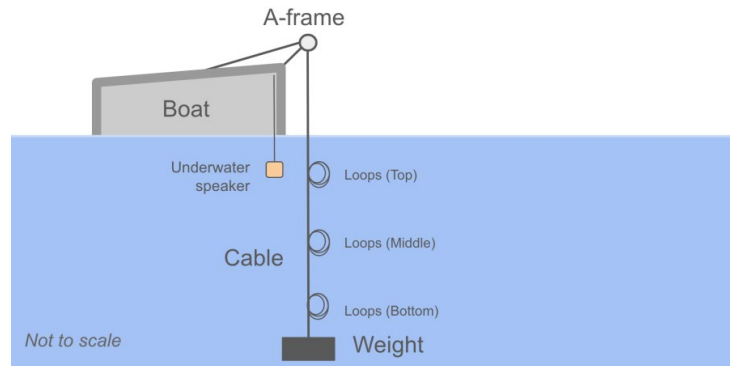
2. Cable Configurations: Different configurations of the sensing cable were tested. Besides the vertical configuration (Figure 19), another setup added a buoy at an intermediate location along the cable to reduce tension, prevent cable entanglement, and keep the end of the fiber away from the boat engine noise (Figure 20). Another configuration involved loops along the cable at different points — top, middle, and bottom — to address cable strain effects and stabilize the cable under different turbulence conditions (Figure 21).

Figure 20: Schematic of Configuration With Buoy at an Intermediate Location Along the Cable



The buoy was used to reduce tension, prevent cable entanglement, and keep the end of the fiber away from boat engine noise.

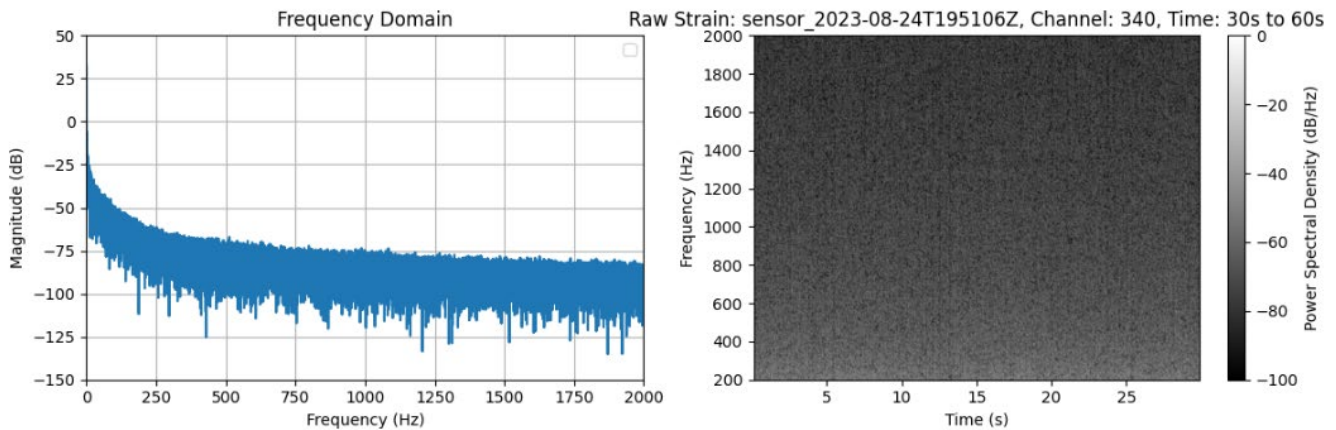
Figure 21: Schematic of Configuration With Loops Along the Cable at Different Depths



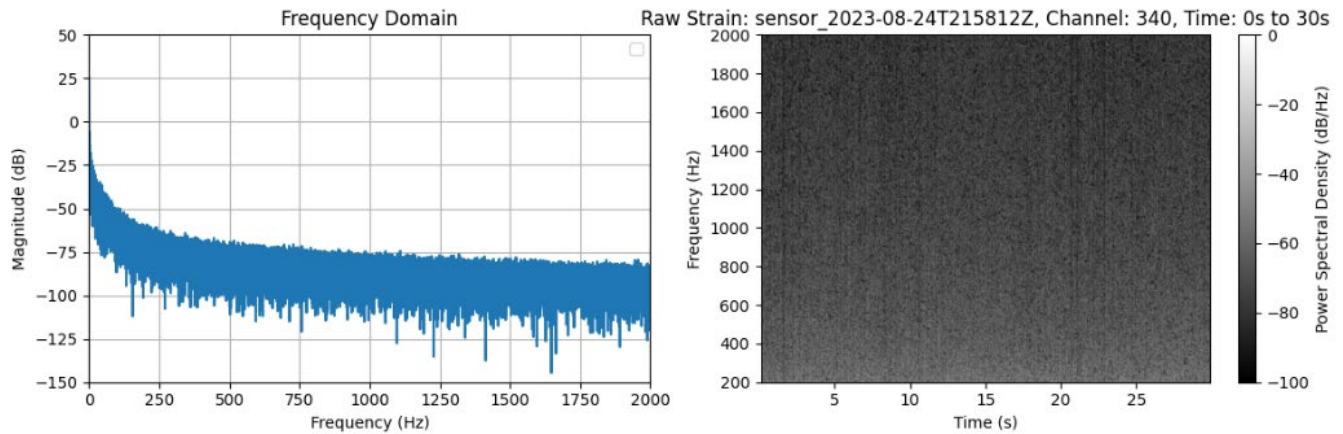
The loops along the cable were installed to address strain effects and stabilize the cable under different turbulence conditions.

When the underwater speaker played a 1,000 Hz tone near the cable, the signal could not be seen in the raw DAS data when the cable was in the vertical configuration (Figure 22, Item 1). The buoy was deployed at an intermediate location with the intention of reducing cable tension and keeping the fiber away from the boat engine noise, but the signal could not be detected (Figure 22, Item 2). When the cable was deployed with three loops along the cable and the engine off, the signal could be seen in the DAS data, with a clear peak at 1000 Hz in the magnitude spectrum and a horizontal line at 1,000 Hz in the spectrogram (Figure 22, Item 3).

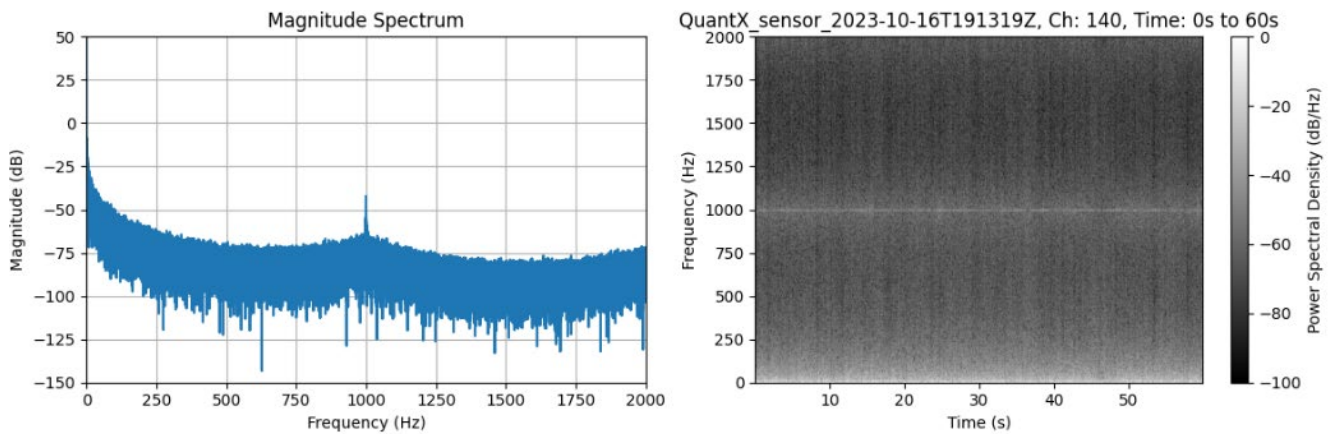
Figure 22: Magnitude Spectra and Spectrograms From the Raw DAS Data



(1) The boat was at the destination point, with the engine on (a cable was placed in the water in a vertical configuration, and a speaker was playing 1,000 Hz near the cable).



(2) The boat was at the destination point, with the engine on (a cable was placed in the water with a buoy at an intermediate location, and a speaker was playing 1,000 Hz near the cable).

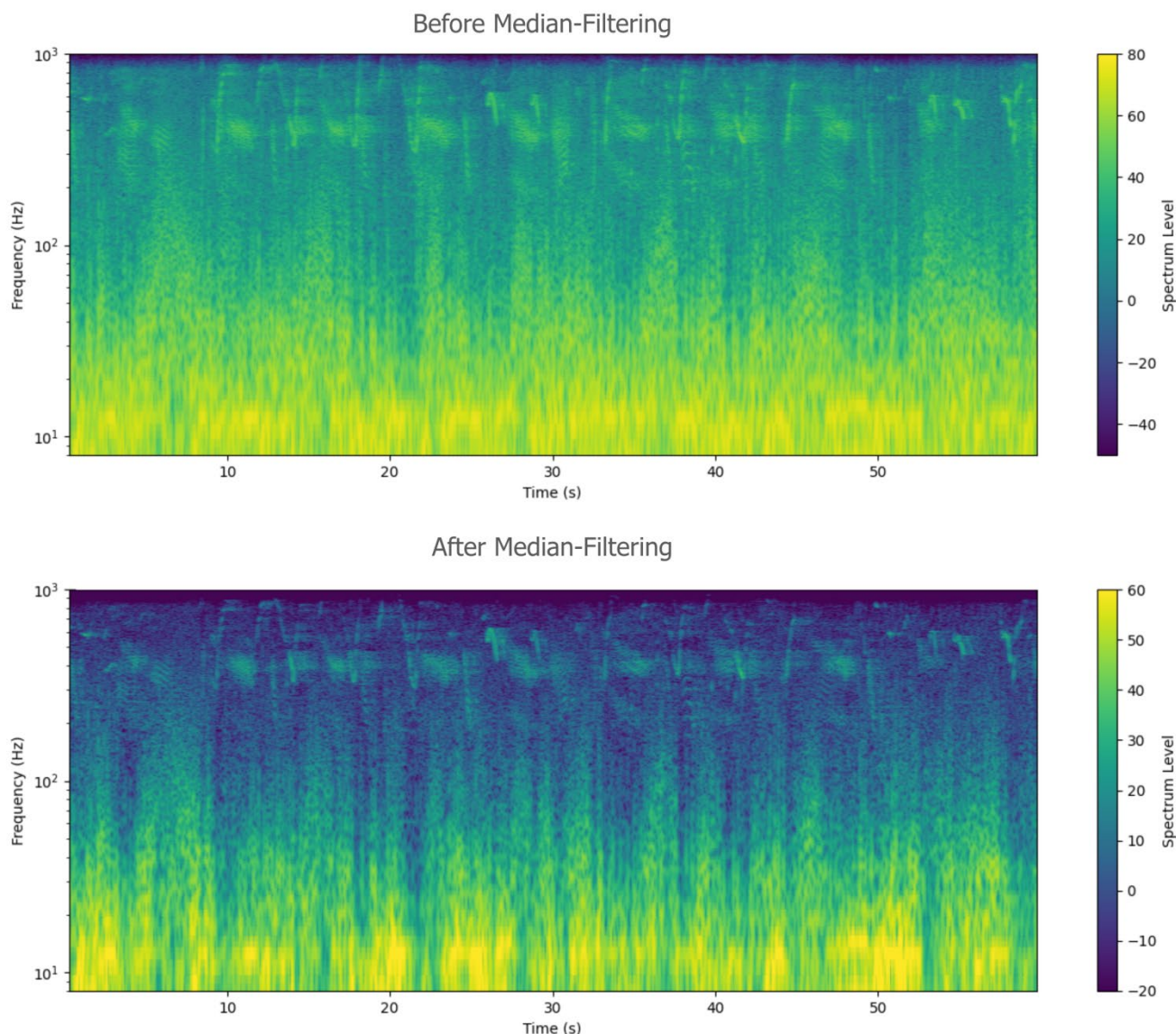


(3) The boat was at the destination point, with the engine off (a cable was placed in the water with loops, and a speaker was playing 1,000 Hz near the cable).

Source: LBNL

3. Median Filtering: Median filtering was used to enhance the quality of DAS data by reducing broadband noise and preserving the integrity of the desired acoustic signals (Figure 23). This technique involves replacing each value in a dataset with the median value of its neighboring values, within a specified window (Justusson, 2006). Median filtering can be effective at removing outliers and noise while retaining important signal features (including whale vocalizations), which may be obscured by random fluctuations.

Figure 23: Spectrogram Generated From DAS Data When a Pre-Recorded Whale Song Was Played on the Underwater Speaker Before and After Median-Filtering



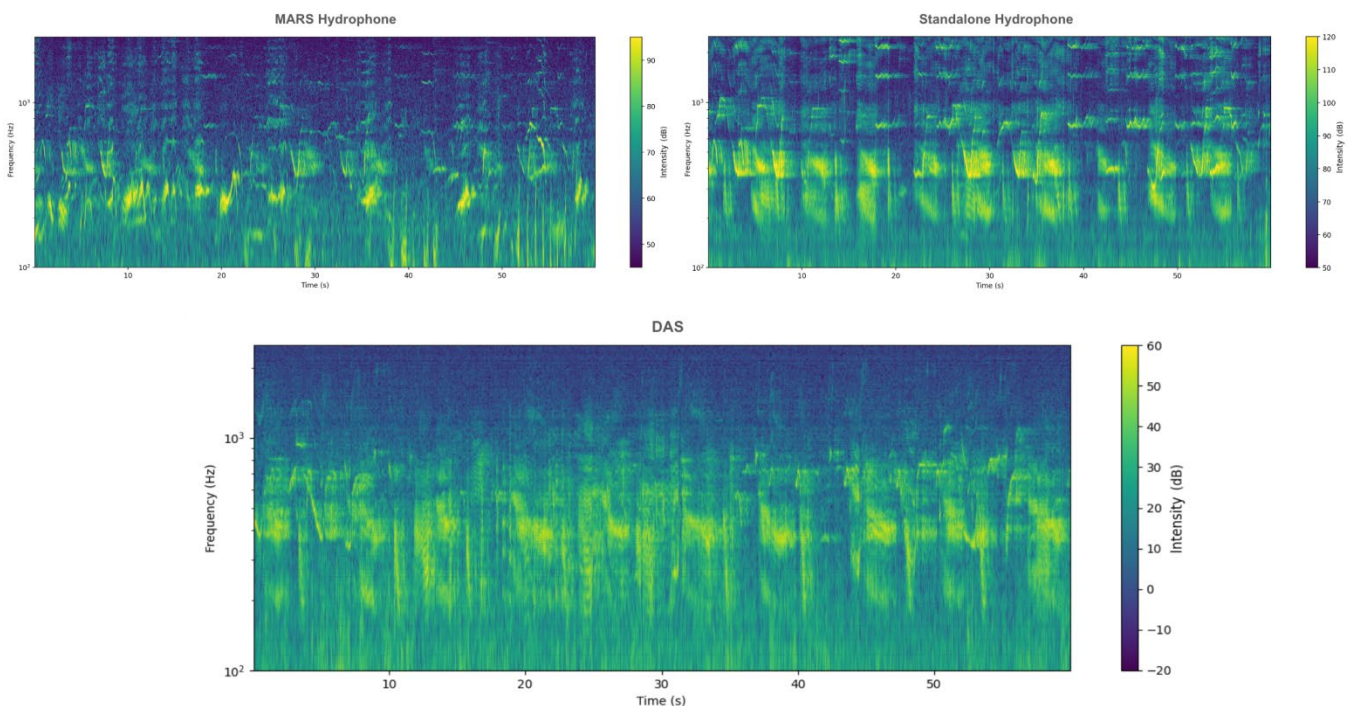
4. Audio Conversion and Cross-Referencing With Hydrophone Audio: To enhance the ability to detect whale vocalizations amidst complex background noise, DAS data were converted into audio files for listening. This conversion was useful because weak or faint vocalizations in the DAS recordings, which might be obscured in spectrograms or other visual representations, could be more readily identified by listening to the audio. These audio data were cross-referenced with data from two hydrophones — one placed along the DAS cable and one placed on the ocean floor — to assess the quality of the DAS audio data. The boat was positioned near an existing Monterey Bay Aquarium Research Institute hydrophone deployed on the ocean floor.

Key Results

Capturing Whale Song Played From Underwater Speaker

A pre-recorded whale song was played from the underwater speaker and recorded by the DAS, a ship-deployed hydrophone, and a sea floor hydrophone. The DAS data (after median filtering and averaging across multiple channels) was then compared with data from the two hydrophones (Figure 24). The ocean floor hydrophone produced high data quality, capturing finer variations in frequency and amplitude, likely due to its stable placement on the ocean floor, which minimized noise interference. The ship-deployed hydrophone, while also effective, showed lower resolution in capturing subtle vocalization features, demonstrating the challenges of monitoring in such a dynamic underwater environment. The DAS system also effectively captured the whale song, although with slightly less resolution than the ship-deployed hydrophone, demonstrating its capability near the sound source. This comparison suggested that the most important factor in determining data quality may not be the distance to the source but rather the interplay of environmental noise and the stability of the sensing system.

Figure 24: DAS Capture of Pre-Recorded Whale Song



When the pre-recorded whale song was played, DAS captured the whale song successfully, while at a higher noise floor than the two hydrophone datasets.

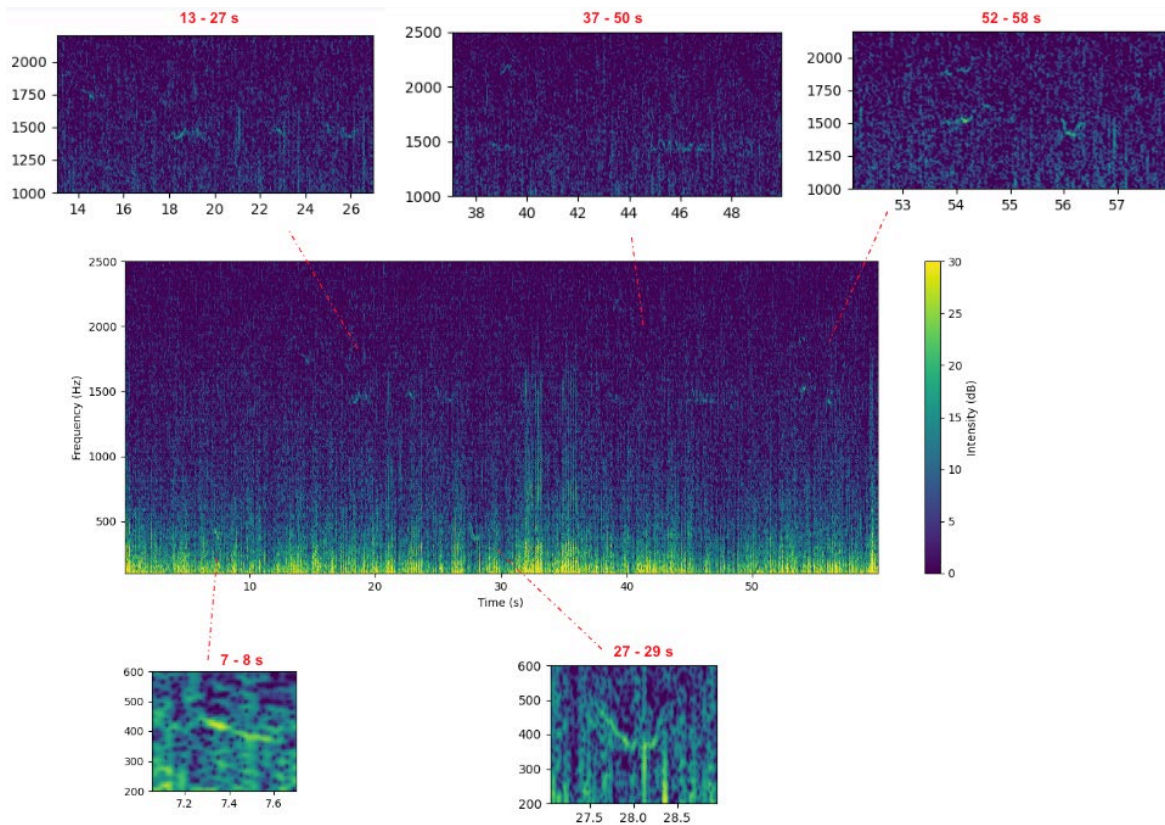
Source: LBNL

Capturing Natural Whale Vocalizations

Natural whale vocalizations were also observed in the DAS data, with the bottom loops in the cable capturing these signals most clearly (Figure 25). Although the surrounding noise sources were lower compared to the controlled speaker-emitted signals, these natural vocalizations

were still discernible. To verify that the spectral features observed in the spectrograms were interpreted correctly, the time series data were converted into audio files. The natural whale vocalizations were confirmed by listening to the converted audio files. The results are promising, given that the noise removal consisted of median filtering, without additional processing.

Figure 25: Examples of Natural Whale Vocalizations Captured by DAS



Source: LBNL

Key points from these experiments follow.

- **DAS Data Quality:** The quality of DAS data was significantly influenced by factors such as boat engine noise, cable configurations, weather conditions, and water turbulence.
- **Noise Challenges:** DAS deployment in shallow-water environments resulted in data with noise that cannot be easily mitigated with conventional signal-processing techniques.
- **Data Comparison:** While DAS data exhibited a higher noise floor compared with hydrophone datasets, the data effectively captured whale vocalizations, particularly when the sound source was close to the sensing cable.
- **Detection of Real Vocalizations:** The DAS system successfully captured controlled whale vocalizations from the speaker. Detecting actual whale calls, which may occur at greater distances from the cable and at lower amplitudes, was more challenging.

CHAPTER 4:

Conclusion

This project advanced the monitoring capabilities of FOSW systems through the development and validation of DFOS technologies. The research enhanced the structural health monitoring of wind towers and gearboxes and environmental impact monitoring on marine mammals through the application of DFOS and DAS technologies. The findings provide valuable insights into integrating advanced sensing technologies into offshore wind applications, offering a pathway to safer, more reliable, and environmentally responsible renewable energy systems.

Key Findings

The project demonstrated significant advancements in the novel use of DFOS technologies to address critical challenges in FOSW monitoring:

1. **Wind Tower Monitoring:** OFDR and ϕ -OTDR technologies enabled high-resolution strain measurements in wind towers under simulated offshore conditions; ϕ -OTDR proved particularly effective for detecting dynamic strain events, providing early detection of structural issues that could impact wind-turbine reliability.
2. **Gearbox Operation Monitoring:** DFOS allowed real-time monitoring of strain distribution under varying load conditions, providing detailed insights into gearbox health. This approach enhanced predictive maintenance strategies, reducing operational costs and improving turbine longevity by enabling early fault detection and accurate torque predictions.
3. **Marine Mammal Detection:** DAS successfully detected whale vocalizations despite noise interference, confirming its potential for monitoring marine life near FOSW installations. The study highlighted the need for improvements in noise mitigation and data processing to optimize DAS effectiveness in real-world applications.

Benefits to California Ratepayers

The results of this project offer direct benefits to California ratepayers by improving the safety, reliability, and environmental sustainability of FOSW systems. The project resulted in proving the ability of DFOS technology to monitor FOSW systems remotely and in real time, which can reduce the need for costly and time-consuming manual inspections and reduce operation and maintenance costs, estimated to be one-third of the LCOE for FOSW systems. Project findings could also minimize the likelihood of system failures, leading to lower energy costs for Californians. Additionally, the proactive maintenance capabilities enabled by DFOS reduce the risk of catastrophic failures, further enhancing reliability and safety. DAS was shown to be capable of monitoring marine mammal presence, potentially leading to improved environmental impact assessments and monitoring abilities. This could lead to faster regulatory approval processes and reductions in project delays, ultimately benefiting ratepayers through more timely and environmentally responsible energy production.

Future Research and Recommendations

Building on the successes of this project, further research is necessary to advance DFOS technologies and unlock their full potential for the FOSW industry. Key areas for future research include the following.

- **Further Development of DFOS Technologies:** There is a need to refine the accuracy and robustness of OFDR and ϕ -OTDR in real-world offshore conditions. Future research should explore optimizing sensor deployment strategies, particularly on floating platforms, and improving strain measurement capabilities under extreme weather conditions. Noise mitigation techniques for DAS require further development to enhance signal clarity, especially in noisy marine environments, enabling better detection of marine mammals.
- **Scaling up Deployment:** Large-scale field tests on commercial FOSW installations are critical for validating the long-term performance of DFOS and DAS under actual operational conditions. Such tests would demonstrate the scalability and cost-effectiveness of these technologies, allowing industry stakeholders to confidently adopt them for broader applications.
- **Integration With Advanced Data Analytics:** The incorporation of machine learning and other data analytics methods into DFOS and DAS technologies is a promising area for future research. These techniques could enhance predictive capabilities by identifying patterns in large datasets, leading to more accurate fault detection and better environmental monitoring.

Strengthening Industry and Academic Collaborations

The results of this project underscore the need for continued collaboration between industry, academic institutions, and regulatory bodies to further advance DFOS technologies. Industry partners, such as California wind energy area developers, can provide real-world testing environments, while academic institutions can drive innovation through ongoing research. Joint research initiatives are particularly important for refining the deployment of monitoring systems on floating platforms and addressing technological challenges. Collaborative efforts, such as co-authored publications and technical exchanges, help bridge the gap between research and commercial applications, accelerating the development of FOSW systems. Research institutions could focus on identifying new materials and methods for improving sensor durability in harsh marine environments.

Engagement With Policymakers

Policymakers play a crucial role in shaping the regulatory framework for FOSW deployment. At this stage, it is important to engage with decision makers such as the Bureau of Ocean Energy Management and the California Coastal Commission (which regulate offshore development) about the potential of DFOS to enhance the safety and environmental stewardship of offshore wind projects. Regulatory bodies should be informed about the capabilities of DFOS for real-time monitoring, which can streamline permitting processes by providing more reliable data on

structural health and environmental impacts. Policymakers also need to consider potential regulatory barriers related to the deployment of advanced sensing technologies, such as data privacy concerns or sensor placements in sensitive marine environments. Addressing these regulatory challenges early can facilitate broader adoption of DFOS technologies to support California's ambitious clean energy mandates.

Conclusion

This project successfully advanced state-of-the-art FOSW monitoring by demonstrating the effectiveness of DFOS technologies in enhancing structural health monitoring and environmental assessments. These outcomes provide a strong foundation for future research, supporting the continued growth of offshore wind as a safe, reliable, and environmentally sustainable source of renewable energy. By building on these achievements and pursuing the recommended actions, DFOS technologies could potentially transform the offshore wind industry, contributing to global efforts to address climate change and achieve a sustainable energy future while benefiting California ratepayers through lower costs, enhanced safety, and environmentally responsible energy production policies.

GLOSSARY AND LIST OF ACRONYMS

Term	Definition
dB	decibel
dB/Hz	decibels per hertz
Distributed Acoustic Sensing (DAS)	A technology that uses optical fibers to detect and measure acoustic signals over long distances. In this project, das was utilized for monitoring marine mammal vocalizations and assessing the environmental impact of floating offshore wind (FOSW) systems.
Distributed Fiber-Optic Sensing (DFOS)	A sensing technology that uses optical fibers to monitor physical changes such as strain, temperature, or acoustic vibrations along the length of the fiber. DFOS provides continuous, high-resolution measurements, making it suitable for monitoring the structural health of wind towers and gearboxes in OWTs.
Floating offshore wind (FOSW)	A type of offshore wind energy technology where wind turbines are mounted on floating platforms anchored to the seabed, allowing deployment in deep ocean waters where traditional fixed-bottom turbines are not feasible.
FOWT	floating offshore wind turbine
Gearbox	A mechanical component in wind turbines that transfers energy from the rotor to the generator. Gearboxes are critical for turbine operation and are often subject to high mechanical loads, making them prone to wear and failure.
Hz	hertz
kHz	kilohertz
kNm	kilonewton meter
kW	kilowatt
lbf	pound force; the weight of one avoirdupois pound at standard gravity
LCOE	levelized cost of energy
m	meter
N	newton
NREL	National Renewable Energy Laboratory
Optical Time Domain Reflectometry (OTDR)	A high-resolution fiber-optic sensing technique that measures strain or temperature along an optical fiber. OTDR provides detailed spatial information by analyzing the backscattered light from the fiber, making it useful for monitoring structural changes in wind towers and other infrastructure.

Term	Definition
Φ -Optical Time Domain Reflectometry (Φ -OTDR)	A type of distributed fiber-optic sensing that measures changes in the phase of light backscattered along an optical fiber. Φ -OTDR is particularly effective for detecting dynamic strain events, such as those caused by wind loading on OWTs.
OWT	offshore wind turbine
PSD	power spectral density
rpm	revolutions per minute
Structural health monitoring (SHM)	The process of implementing a damage detection and characterization strategy for structures such as wind towers and gearboxes. SHM involves the continuous monitoring of a structure's health to ensure its safety, reliability, and longevity.
$\mu\epsilon$	microstrain
$\mu\epsilon^2/\text{Hz}$	microstrains per hertz
Wind tower	The vertical structure that supports the nacelle and rotor of a wind turbine. In OWTs, the tower must withstand significant environmental loads, making structural health monitoring essential for safe operation.

References

- Bailey, Helen, Bridget Senior, Dave Simmons, Jan Rusin, Gordon Picken, and Paul M. Thompson. 2010. "[Assessing underwater noise levels during pile-driving at an offshore windfarm and its potential effects on marine mammals](#)." *Marine Pollution Bulletin*, 60(6): 888–897. Available at <https://doi.org/10.1016/j.marpolbul.2010.01.003>.
- Bouffaut, Léa, Kittinat Taweessintananon, Hannah Kriesell, Robin Rørstadbotnen, John Potter, Martin Landrø, Ståle Johansen, Jan Brenne, Aksel Haukanes, Olaf Schjelderup, and Frode Storvik. 2022. "[Eavesdropping at the Speed of Light: Distributed Acoustic Sensing of Baleen Whales in the Arctic](#)." *Frontiers in Marine Science*, 9. Available at <https://doi.org/10.3389/fmars.2022.901348>.
- Grattan, Kenneth, and B. Meggitt. 2000. *Optical Fiber Sensor Technology: Advanced Applications - Bragg Gratings and Distributed Sensors*, vol. 5. Springer Nature B.V., United States. 1–400. ISBN: 9780792379461.
- Gutierrez Santiago, Unai, Alfredo Fernández Sisón, Henk Polinder, and Jan-Willem van Wingerden. 2022. "[Input torque measurements for wind turbine gearboxes using fiber-optic strain sensors](#)." *Wind Energy Science*, 7(2): 505–521. Available at <https://doi.org/10.5194/wes-7-505-2022>.
- Hubbard, Peter G., James Xu, Shenghan Zhang, Matthew Dejong, Linqing Luo, Kenichi Soga, Carlo Papa, Christian Zulberti, Demetrio Malara, Fabio Fugazzotto, Francisco Garcia Lopez, and Chris Minto. 2021. "[Dynamic Structural Health Monitoring of a Model Wind Turbine Tower Using Distributed Acoustic Sensing \(DAS\)](#)." *Journal of Civil Structural Health Monitoring*, 11(3): 833–849. Available at <https://doi.org/10.1007/s13349-021-00483-y>.
- Justusson, B. I. 2006. "[Median Filtering: Statistical Properties](#)." In *Two-Dimensional Digital Signal Processing II: Transforms and Median Filters. Topics in Applied Physics*, vol. 43: 161–196. Springer. <https://doi.org/10.1007/BFb0057597>.
- Keller, Jonathan, Yi Guo, Zhiwei Zhang, and Doug Lucas. 2017. [Planetary Load Sharing in Three-Point Mounted Wind Turbine Gearboxes: A Design and Test Comparison](#). National Renewable Energy Laboratory. Report Number: NREL/TP-5000-67394. Available at <https://www.nrel.gov/docs/fy17osti/67394.pdf>.
- Lindsey, Nathaniel J., T. Craig Dawe, and Jonathan B. Ajo-Franklin. 2019. "[Illuminating Seafloor Faults and Ocean Dynamics With Dark Fiber Distributed Acoustic Sensing](#)." *Science*, 366(6469): 1103–1107. Available at <https://doi.org/10.1126/science.aay5881>.
- Luna Innovation Inc. 2018. "[ODiSI 6100 Optical Distributed Sensor Interrogator](#)." Available at https://web.archive.org/web/20180403141124/http://lunainc.com/wp-content/uploads/2017/11/ODB6_DataSheet_v2_rev1-0-2.pdf.
- Madsen, Peter T., Magnus Wahlberg, Jakob Tougaard, and Klaus Lucke. 2006. "[Wind Turbine Underwater Noise and Marine Mammals: Implications of Current Knowledge and Data](#)

[Needs](https://doi.org/10.3354/meps309279)." *Marine Ecology Progress Series*, 309: 279–295. Available at <https://doi.org/10.3354/meps309279>.

Matsumoto, Hiroyuki, Eiichiro Araki, Toshinori Kimura, and Gou Fujie. 2021. "[Detection of Hydroacoustic Signals on a Fiber-Optic Submarine Cable](#)." *Scientific Reports*, 11(1), 2797. Available at <https://doi.org/10.1038/s41598-021-82093-8>.

Romanowicz, Barbara, Richard Allen, Knute Brekke, Li-Wei Chen, Yuancong Gou, Ivan Henson, Julien Marty, Doug Neuhauser, Brian Pardini, Taka'aki Taira, Stephen Thompson, Junli Zhang, and Stephane Zuzlewski. 2023. "[SeaFOAM: A Year-Long DAS Deployment in Monterey Bay, California](#)." *Seismological Research Letters*, 94(5): 2348–2359. Available at <https://doi.org/10.1785/0220230047>.

Rosinski, Jarek, and David Smurthwaite. 2010. "[Troubleshooting Wind Gearbox Problems](#)." Accessed June 11, 2023. Available at https://web.archive.org/web/20240513082457/https://gearsolutions.com/media/uploads/uploads/assets/PDF/Articles/Feb_10/0210_JR_dynamics.pdf.

SEAFOM Fiber Optic Monitoring Group. 2018. [Measuring Sensor Performance Document – 02 \(SEAFOM MSP-02\): DAS Parameter Definitions and Tests](#). IOP Publishing, UK. August, 2018. Available at <https://studylib.net/doc/27316805/measuring-sensor-performance>.

Taweesintananon, Kittinat, Martin Landrø, Jan Kristoffer Brenne, and Aksel Haukanes. 2021. "[Distributed Acoustic Sensing for Near-Surface Imaging Using Submarine Telecommunication Cable: A Case Study in the Trondheimsfjord, Norway](#)." *Geophysics*, 86(5): B303–B320. Available at <https://doi.org/10.1190/geo2020-0834.1>.

Wilcock, William S. D., Shima Abadi, and Bradley P. Lipovsky. 2023. "[Distributed Acoustic Sensing Recordings of Low-Frequency Whale Calls and Ship Noise Offshore Central Oregon](#)." *JASA Express Letters*, 3(2). <https://doi.org/10.1121/10.0017104>.

Xu, James, Linqing Luo, Jaewon Saw, Chien-Chih Wang, Sumeet Sinha, Ryan Wolfe, Kenichi Soga, Yuxin Wu, and Matthew Dejong. 2023. "[A Shake-Table Test to Evaluate Fiber Optic Vibration Monitoring of Offshore Wind Turbines](#)." In Limongelli, M. P., P. F. Giordano, S. Quqa, C. Gentile, and A. Cigada (eds.), *Experimental Vibration Analysis for Civil Engineering Structures*. EVACES 2023. *Lecture Notes in Civil Engineering*, 432: 242–251. Cham: Springer Nature Switzerland. Available at https://doi.org/10.1007/978-3-031-39109-5_25.

Zhang, Hongkun, Rubén Ortiz de Luna, Martin Pilas, and Jan Wenske. 2018. "[A Study of Mechanical Torque Measurement on the Wind Turbine Drive Train — Ways and Feasibilities](#)." *Wind Energy*, 21(12): 1239–1449. Available at <https://doi.org/10.1002/we.2263>.

Project Deliverables

Project Deliverables are listed below. These project deliverables, including interim project reports, are available upon request by submitting an email to pubs@energy.ca.gov.

- Tech Evaluation Report
- Test Facility Design And Construction Report
- Numerical Development Report #1
- Numerical Development Report #2
- Field Test Plan
- Field Test Status Report
- Field Test Report
- Benefit Questionnaires
- Tech Transfer Plan
- Tech Transfer Report
- Production Readiness Plan
- Presentation Material
- High Quality Photographs
- Final Project Report (This Report)



**CALIFORNIA
ENERGY COMMISSION**



ENERGY RESEARCH AND DEVELOPMENT DIVISION

APPENDIX A: Data Summary Table

May 2025 | CEC-500-2025-023



Appendix A:

Data Summary Table

The table below summarizes the main datasets generated during this project. These datasets are available upon request from the lead author of this report. The table describes the types of data available, data format, description of the data and the main parameters of each dataset.

Table A-1: Distributed Strain and Temperature Sensing (including Wind Turbine Structure Tests and Gearbox Monitoring Tests)

TERM	DESCRIPTION
DATA STRUCTURE	The data is stored in multiple files for each test to limit individual file sizes to under 2 GB.
DATA FORMATTING	Files are in .tsv format.
DATA DESCRIPTION	Rows represent recording time, and columns represent distance. The data begins at row 34, with the baseline at row 32.
DATA PARAMETERS	Sampling rate and spatial resolution are stored in the header of each file.

Table A-2: Distributed Acoustic Sensing (including Wind Turbine Structure Tests and Whale Calling Recording Tests)

TERM	DESCRIPTION
DATA STRUCTURE	Data is saved every minute, with each file representing one minute of recordings.
DATA FORMATTING	Files are in h5 format. The data matrix is located at /Acquisition/Raw[0]/RawData, and the corresponding time is found at /Acquisition/Raw[0]/RawDataTime.
DATA DESCRIPTION	Data is organized as a matrix, where rows represent time and columns represent distance.
DATA PARAMETERS	Sampling rate and spatial resolution are included in the header of each h5 file. The wind turbine structure test data was recorded at 1 kHz, and whale calling data was recorded at 10 kHz.

Example MATLAB Code for Data Analysis:

- **Reading Strain Data (.tsv file):**

An example MATLAB code snippet for reading strain data from a .tsv file is provided below. The matrix CoilD4 contains strain information, obtained from channel 2 (ch2) in spectral shift (GHz). Before processing, the data is converted to strain by multiplying by a coefficient of 6.67. The recorded time is initially in UTC and has been converted to local time.

- **Plotting Acoustic Data in Different Bandwidth Windows:**

A MATLAB code example for opening and plotting acoustic data across different bandwidth windows is also provided. The bandwidth windows are specified as follows: 0.1-0.2, 0.2-0.4, 0.4-1, 1-2, 2-4, 4-8, 8-16, 16-32, 32-64, 64-128, 128-256, and 256-512 Hz. The primary function for reading the h5 file is "h5read". The data time, stored in UTC, can be converted to any required time zone.

Strain data example code:

```
files = dir('*ch2_full.tsv');
for n=7:1:7
    for m=1:1
        inx=n;%(n-1)*2+m;
        datatable = readtable(files(inx).name,'ReadVariableNames', true,'FileType','text');
        numRows = height(datatable);
        numCols = width(datatable);
        delete datatable;
        D4=readmatrix(files(inx).name,'Range',[34 4 numRows numCols],'FileType','text');
        distance4=readmatrix(files(inx).name,'Range',[33 4 33 numCols],'FileType','text');
        TimeUTC4=readmatrix(files(inx).name,'Range',[34 1 numRows 1],'FileType','text','Outputtype','datetime');
        time4=datetime(TimeUTC4,'TimeZone','UTC');
        time4.TimeZone='Europe/Madrid';

        strain=D4-D4(1,:); %spectral shift (GHz)
        CoilD4=gpuArray(strain(:,:)*-6.67);
        disCoil4=distance4(:);
        time=datenum(time4);
```

Acoustic data example code:

```
clear all; close all; clc
%% change parameters
nchan0= 150;
ch1=80;
ch2=140;
dnameout1='F:\06092022_BOAT_TEST\Cable1_SPEAKER__2022-06-09T12_36_44-0700\Plots';
files = dir('Cable1*.h5');
%%
fbands=[
    0.1 0.2
    0.2 0.4
    0.4 1
    1 2
    2 4
    4 8
```

```

8 16
16 32
32 64
64 128
128 256
256 512
];
nbands=size(fbands,1);
fstrlist={'0.1-0.2','0.2-0.4','0.4-1','1-2','2-4','4-8','8-16','16-32','32-64','64-128','128-256','256-512'};

timedomain=[
    {1:4}
];

dx0=1;
x1=(0:nchan0-1).*dx0;
GL = h5readatt(files(1).name, '/Acquisition', 'GaugeLength');
fs = 1.*h5readatt(files(1).name, '/Acquisition', 'PulseRate');
dt = 1/fs;
fs1=fs;

% [numrows, numcols] = getdims(files(1));
% t0 = 0:dt:(dt*double(numrows)) - dt_;

%figure setting
posx=0.06;
fw=0.9;
fh=0.88;
posy=1-fh-0.045;
fn1=18;
npts0=fs*60*5;
npts1=fs1*60*5;
dt0=dt;
dt1=dt0;

fnum = 0;
for m=1:length(timedomain)
    Rawmtx=[];
    a1=[];
    for i = timedomain{m} %36:42%length(files)

        fnum = fnum + 1;
        fname = files(i).name;
        Rawmtx1 = h5read(fname, '/Acquisition/Raw[0]/RawData');
        RawDataTime = h5read(fname, '/Acquisition/Raw[0]/RawDataTime');
        Rawmtx=[Rawmtx;Rawmtx1];
    end
end

```

```

a1=double((Rawmtx-Rawmtx(1,:)));
%a1=1550*(a1.*pi./2^15)./(4*pi*1.465*GL*10^9*0.78)*10^9;

alim2=quantile(a1(ch1:ch2,:),0.95,[1 2]);
%alim3=max(abs(a1(50:70,:)),[1 2]);
t0 = 0:dt:(dt*double(length(a1(1,:))) - dt);
figure('units','normalized','position',[0 0 1 1],'visible','off');
    subplot('Position',[posx posy fw fh]);
    imagesc(x1,t0,a1');
    colormap(jet);
    caxis(alim2.*[-1 1]);
    hcb=colorbar;
    set(hcb,'fontsize',fn1);
    %text(20,80,[num2str(alim3,'%1e')],'fontsize',fn1);
    %text(-1,92,[evid(1:end-3)'],'h5ot','M: ',num2str(eqmat(idx,5),'%.2f'),' depth:
        ',num2str(h5depth,'%1f'),' km, dist: ',num2str(min(hdist),'%.1f'),'-',num2str(max(hdist),'%.1f'),' km,
        Raw'],'fontsize',fn1);
    set(gca,'YDir','normal','fontsize',fn1);
    xlabel('Optical Distance (m)','fontsize',fn1);
    ylabel('Time (s)','fontsize',fn1);

fname2=[dnameout1,'\',files(i).name,'_0.png'];
set(gcf,'PaperPositionMode','auto');
print(gcf,'-dpng','-r150',fname2);
close(gcf);

npts0=fs*60*length(timedomain{m});
npts1=fs1*60*length(timedomain{m});
ctap0=tukeywin(npts0,min([0.04 5/(npts0*dt0)]));
ctap0=ctap0';
ctap1=tukeywin(npts1,min([0.04 5/(npts1*dt1)]));
ctap1=ctap1';

a2=bsxfun(@minus,a1,median(a1(ch1:ch2,:),1));
amat2=[];
amat3=[];
for rc1=1:nchan0
    %atemp=double(a1(rc1,:));
    atemp=a2(rc1,:);
    atemp=detrend(atemp);
    atemp=atemp.*ctap0;
    %atemp=decimate(atemp,2);
    %atemp=detrend(atemp).*ctap1;

    % INTEGRATING
    % atemp=dt0*cumtrapz(atemp);
    % atemp=filtfilt(bfsos1,bfg1,atemp);

```

```

amat2(rc1,:)=atemp;

end
for rc1=1:nchan0
    amat2(rc1,:)=detrend(amat2(rc1,:)).*ctap1;
end
amat3=amat2;

% FOR A RANGE OF PASSBANDS

for rc3=1:nbands

    % DEFINE THE FILTER, [10 20], [20 40], fs1=Niquist frequency
    [bfz1,bfp1,bfk1]=butter(2,fbands(rc3,:)./(fs1/2),'bandpass');
    [bfsos1,bfg1]=zp2sos(bfz1,bfp1,bfk1);
    Hd_bf1=dfilt.df2sos(bfsos1,bfg1);
    % FOR EACH CHANNEL FILERING
    for rc1=1:nchan0
        atemp=double(amat3(rc1,:));
        atemp=filtfilt(bfsos1,bfg1,atemp);
        amat2(rc1,:)=atemp;
    end
    % SET COLOR SCALE
    alim2=quantile(amat2(ch1:ch2,:),0.8,'all');
    % PLOTTING
    figure('units','normalized','position',[0 0 1 1],'visible','off');
    subplot('Position',[posx posy fw fh]);
    imagesc(x1,t0,amat2');
    colormap(jet);
    caxis(alim2.*[-1 1]);
    hcb=colorbar;
    set(hcb,'fontsize',fn1);
    %text(-1,92,[evid(1:end-3),' ',h5ot,' M: ',num2str(eqmat(idx,5),'%0.2f'),', depth: ',
    num2str(h5depth,'%0.1f'),' km, dist: ',num2str(min(hdist),'%0.1f'),'-',num2str(max(hdist),'%0.1f'),' km, ',
    fstrlist{rc3},' Hz'],'fontsize',fn1);
    set(gca,'YDir','normal','fontsize',fn1);
    xlabel('Optical Distance (km)','fontsize',fn1);
    ylabel('Time (s)','fontsize',fn1);
    fname2=[dnameout1,'\',files(i).name,'_',num2str(rc3),'.png'];
    set(gcf,'PaperPositionMode','auto');
    print(gcf,'-dpng','-r150',fname2);
    close(gcf);
end
end

```